Ş. Oğuzhan TEKDEN

M.Sc. Thesis

AGU 2025

THERAPEUTIC TARGETING OF SYK IN AML: *In Silico* DRUG REPURPOSING and FUNCTIONAL VALIDATION of BI 1002494

M.Sc. THESIS
SUBMITTED TO THE DEPARTMENT OF BIOENGINEERING
AND THE GRADUATE SCHOOL OF ENGINEERING AND SCIENCE
OF ABDULLAH GUL UNIVERSITY
IN PARTIAL FULFILLMENT OF THE REQUIREMENTS
FOR THE DEGREE OF
MASTER OF SCIENCE

By
Şevket Oğuzhan TEKDEN
July 2025

THERAPEUTIC TARGETING OF SYK IN AML: *In Silico* DRUG REPURPOSING and FUNCTIONAL VALIDATION of BI 1002494

A THESIS
SUBMITTED TO THE DEPARTMENT OF BIOENGINEERING
AND THE GRADUATE SCHOOL OF ENGINEERING AND SCIENCE OF
ABDULLAH GUL UNIVERSITY
IN PARTIAL FULFILLMENT OF THE REQUIREMENTS
FOR THE DEGREE OF
MASTER OF SCIENCE

By
Şevket Oğuzhan TEKDEN
July 2025

SCIENTIFIC ETHICS COMPLIANCE

I hereby declare that all information in this document has been obtained in accordance with academic rules and ethical conduct. I also declare that, as required by these rules and conduct, I have fully cited and referenced all materials and results that are not original to this work.

Name-Surname: Şevket Oğuzhan TEKDEN

Signature :

REGULATORY COMPLIANCE

M.Sc. thesis titled Therapeutic Targeting of Syk in AML: In silico Drug Repurposing and Functional Validation of BI 1002494 has been prepared in accordance with the Thesis Writing Guidelines of the Abdullah Gül University, Graduate School of Engineering & Science.

Prepared By	Advisor	Co Advisor
Şevket Oğuzhan TEKDEN	Asst. Prof. Emel Başak GENCER AKÇOK	Asst. Prof. İsmail AKÇOK
Signature	Signature	Signature

Head of the Bioengineering Program

Asst. Prof. İsmail AKÇOK

Signature

ACCEPTANCE AND APPROVAL

M.Sc. thesis titled Therapeutic Targeting of Syk in AML: In silico Drug Repurposing and Functional Validation of BI 1002494 and prepared by Şevket Oğuzhan TEKDEN has been accepted by the jury in the Bioengineering Graduate Program at Abdullah Gül University, Graduate School of Engineering & Science.

…….. /…….. / ……..

(Thesis Defense Exam Date)

JURY:

Advisor : Asst. Prof. Emel Başak GENCER AKÇOK

Member : Asst. Prof. Şerife AYAZ GÜNER

Member : Asst. Prof. Sibel SARI TÜRK

APPROVAL:

The acceptance of this M.Sc. thesis has been approved by the decision of the Abdullah Gül University, Graduate School of Engineering & Science, Executive Board dated ….. /….. / …….. and numbered ……..……. .

…….. /…….. / ……..

(Date)

Graduate School Dean
Prof. İrfan ALAN

ABSTRACT

THERAPEUTIC TARGETING OF SYK IN AML: *In Silico* DRUG REPURPOSING and FUNCTIONAL VALIDATION of BI 1002494

Şevket Oğuzhan TEKDEN
MSc. in Bioengineering
Advisor: Asst. Prof. Emel Başak GENCER AKÇOK
Co-advisor : Asst. Prof. İsmail AKÇOK
July 2025

Acute myeloid leukemia (AML) is a blood cancer type characterized by the uncontrolled growth and proliferation of myeloid cells in the bone marrow. Although methods such as radiotherapy are used for treatment, limited success rates necessitate other targeted treatment studies. The spleen tyrosine kinase (Syk) enzyme, known to be associated with AML, is an enzyme important in intracellular signaling. Disorders that may occur in Syk are highly effective in the AML emergence. Therefore, inhibitors focusing on Syk are promising for AML. In the study, *in silico* molecular docking was performed on a candidate molecule in the opnMe database, Syk inhibitor "BI 1002494", showing high binding affinity, was selected, and a targeted "drug repurposing" was performed for Syk. The catalytic domain of Syk was produced by recombinant methods using *Escherichia coli* bacteria, the catalytic domain was purified by His-tag Ni-NTA affinity chromatography method and the presence of the purified protein was confirmed by Western Blot (WB) method, and Thermal Shift Assay (TSA) experiments were performed to investigate the effects of the inhibitor on the protein at the molecular level. For the cellular activity, MTT cytotoxicity assays were performed on MOLM-13 and K562 cell lines and it was observed that BI 1002494 suppressed cell proliferation, and the acquired data were similar to the FDA-approved drug R406. The results indicate that BI 1002494 is a potential therapeutic Syk inhibitor against AML. This study provides valuable contributions to targeted, *in silico* therapeutic approaches in the drug repurposing context.

Keywords: AML, Syk, drug repurposing, recombinant DNA, inhibitor

ÖZET

AKUT MİYELOİD LÖSEMİDE SYK ENZİMİNİN HEDEFLENMESİ: BI 1002494'ÜN *In Silico* İLAÇ YENİDEN KONUMLANDIRIMI ve İŞLEVSEL DOĞRULAMASI

Şevket Oğuzhan TEKDEN
Biyomühendislik Anabilim Dalı Yüksek Lisans
Tez Danışmanı: Dr. Öğretim Üyesi Emel Başak GENCER AKÇOK
İkinci Tez Danışmanı: Dr. Öğretim Üyesi İsmail AKÇOK
Temmuz 2025

Akut miyeloid lösemi (AML), kemik iliğindeki miyeloid hücrelerin denetimsiz biçimde büyümesi ve çoğalmasıyla tanımlanan bir kan kanseri türüdür. Sağaltım için radyoterapi gibi yöntemlere başvurulsa da bunların sınırlı başarı oranlarına iye olması, başka hedefe yönelik sağaltım çalışmalarını zorunlu kılmaktadır. AML ile ilişkili olduğu bilinen dalak tirozin kinaz (Syk) enzimi hücre içi sinyal iletiminde önemli bir enzimdir. Syk'de oluşabilecek bozukluklar, AML'nin ortaya çıkması üzerinde oldukça etkilidir. Bu nedenle Syk odaklı kullanılan inhibitörler AML açısından umut vericidir. Çalışmada opnMe veri tabanındaki aday molekül üzerinde *in silico* moleküler kenetleme gerçekleştirilmiş ve yüksek bağlanma eğilimi gösteren "BI 1002494" Syk inhibitörü seçilerek, hedefe yönelik bir "ilaç yeniden konumlandırma" gerçekleştirilmiştir. Syk'nin katalitik bölgesi, *Escherichia coli* bakterilerinde rekombinant olarak üretilmiş ve His-işaretli Ni-NTA afinite kromatografi yöntemi ile katalitik bölge saflaştırılmıştır. Saflaştırılan proteinin varlığı Western Blot (WB) yöntemiyle doğrulanmış ve Termal Kayma Deneyi (TSA) ile inhibitörün protein üzerindeki moleküler düzeyde etkileri araştırılmıştır. Hücresel etkinlik tespiti için, MOLM-13 ve K562 hücre hatlarında MTT sitotoksisite deneyleri gerçekleştirilmiş, BI 1002494'ün hücre çoğalmasını baskıladığı, elde edilen verilerin FDA onaylı Syk inhibitörü R406 ile benzer düzeylerde olduğu gözlemlenmiştir. Sonuçlar, BI 1002494'ün AML'ye karşı olası sağaltıcı bir Syk inhibitörü olduğunu göstermektedir. Bu çalışma, ilaç yeniden konumlandırma kapsamında hedefe odaklı, bilgisayar tabanlı sağaltım yaklaşımlarına değerli katkılar sunmaktadır.

Anahtar sözcükler: AML, Syk, ilaç yeniden konumlandırma, rekombinant DNA, inhibitör

Acknowledgements

First of all, special regards to Asst. Prof. Emel Başak GENCER AKÇOK and, who has become my advisor from the beginning of my master program. I have always been proud to be her student and I sincerely express my regards to her since she has constantly communicated with me and has built my motivation during the whole process.

I also would like to send my regards to my co-advisor Asst. Prof. İsmail AKÇOK for sharing his experiences and laboratory resources during the experiments.

I would like to thank to my thesis defense jury members; Asst. Prof. Şerife AYAZ GÜNER and Asst. Prof. Sibel SARI TÜRK for their valuable contributions.

Besides, I will always be grateful to my guides Merve ŞANSAÇAR and Özkan İLMEK, who never spared their help and their time when I had challenges during the experiences, for their efforts.

I would like to thank my friends Muhsin Samet YÜCEL, Beyza Nur DEMİRSOY, Dudu BOVYAT and Fatma FINDIK, and my former teacher Asst. Prof. Şerife AYAZ GÜNER, who guided me with their experiences and never withheld their suggestions for the difficulties I encountered during the experiments, from long distances.

I would also like to thank Abdullah Gül University for supporting me during the whole process with the resources needed.

Finally and most importantly, I am completely grateful to my beloved family, who have been my biggest supporters throughout my entire life. Their infinite support, belief and advices towards me have always been the most valuable factors in my life. That’s why, I send my deep love to my mother, my father, my sisters and my beautiful fiancé, who have always given me strength I need.

TABLE OF CONTENTS

LIST OF FIGURES

LIST OF TABLES

LIST OF ABBREVIATIONS

ADME	Absorption, Distribution, Metabolism and Excretion
AML	Acute Myeloid Leukemia
ATP	Adenosine Triphosphate
BCA	Bicinchoninic Acid Assay
BCR	B-Cell Receptor
CML	Chronic Myeloid Leukemia
DMSO	Dimethyl Sulfoxide
DNA	Deoxyribonucleic Acid
ECL	Electrochemiluminescence
ERK	Extracellular Signal-Regulated Kinase
FDA	Food and Drug Administration
GAPDH	Glyceraldehyde 3-Phosphate Dehydrogenase
HEPES	2-(4-(2-Hydroxyethyl)-1-Piperazinyl)-Ethanesulfonic Acid
IC	Inhibitory Concentration
PDB	Protein Data Bank
IMAC	Immobilized Metal Affinity Chromatography
IPTG	Isopropyl-β-d-Thiogalactopyranoside
ITAM	Immunoreceptor Tyrosine-Based Activation Motif
JAK	Janus Kinase
LB	Lysogeny Broth
MTT	3-(4,5-Dimethylthiazol-2-yl)-2,5-Diphenyltetrazolium Bromide
NF-κB	Nuclear Factor Kappa-Light-Chain-Enhancer of Activated B Cells
OD	Optical Density
PCR	Polymerase Chain Reaction
PPI	Protein-Protein Interaction
RPMI	Roswell Park Memorial Institute
PVDF	Polyvinylidene Fluoride
QSAR	Quantitative Structure-Activity Relationship
RAS	Rat Sarcoma Virus
RIPA	Radioimmunoprecipitation Assay
RNA	Ribonucleic Acid

SDS	Sodium Dodecyl Sulfate
Syk	Spleen Tyrosine Kinase
TAE	Tris-Acetate-EDTA
TBST	Tris-Buffered Saline with 0.1% Tween 20 Detergent
TSA	Thermal Shift Assay
WB	Western Blot

Chapter 1

Introduction

1.1 Acute Myeloid Leukemia

Acute myeloid leukemia (AML) is a type of blood cancer characterized by the accumulation of myeloid cells in the bone marrow and blood circulation that have not completed their differentiation. The cells possess various mutations in their genome and the epigenetic mechanisms may also vary from patient to patient, as well. Although it is especially common in adults, promising treatment rates are reported with immediate action after diagnosis [1].

Genetic mutations such as DNMT3A, NPM1, IDH1/2 and FLT3 stand out in the development and spread of AML. These mutations contribute to the increased cell proliferation, while simultaneously preventing differentiation and suppressing apoptosis [2]. Moreover, abnormalities in epigenetic regulators such as DNMT3A can promote leukemogenesis by affecting gene expression through DNA methylation [3]. In AML, uncontrolled activation of proliferative cell signaling pathways, including PI3K/AKT, RAS/MAPK, and JAK/STAT, are frequently associated with these mutations. These pathways not only increase cell survival but also confer resistance against treatment modalities such as chemotherapy [4].

Treatment regimens including cytarabine often appear to have limited success rates, and are accompanied by the constant risk of disease relapse. This is especially evident in drug-resistant AML subtypes, where overexpression of BCL2-like apoptosis suppressor proteins and uncontrolled activation of DNA repair pathways are commonly observed [5]. In recent studies, targeted therapies have come to the fore. Although inhibitors targeting specific genetic alterations such as FLT3, BCL2 and IDH1/2 have been shown to be successful in selected patient groups, the effect of these methods in terms of the general

patient profile is still an issue that needs to be studied and requires further investigation. This highlights the need to identify the non-mutation dependent targets that are more comprehensively related to the solution of the AML pathogenesis [6].

Considering all these, kinases involved in cell signaling, such as Spleen Tyrosine Kinase (Syk), stand out as possible targets. Cell signaling pathway molecules such as Syk appear to be involved in multiple apoptotic and proliferative events, not just one, and are therefore considered to be among the versatile targets that could reduce the likelihood of drug resistance [7]. Syk appears to be directly involved in anti-apoptotic and proliferative signals in AML cells, not only through its interactions with immune cell-related signaling pathways but also with PI3K/AKT and RAS/MAPK. Cross-activation of these pathways appears to contribute to the emergence of a treatment-resistant strain [8]. Due to its role in promoting survival signals and uncontrolled activation of AML cells, Syk enzyme has become the focus of study. Accordingly, studies aiming to inhibit Syk or controlling its activity are undoubtedly of great importance in the development of more effective and novel treatment methods.

Given the complexity of the signaling networks involved in AML, it is increasingly understood that single molecular targets do not function adequately on their own. Instead, they function within multilayered protein-protein interaction (PPI) networks that regulate fundamental cellular processes such as proliferation, apoptosis, and differentiation. Disruptions or reprogramming in these PPI networks significantly contribute to leukemogenesis and therapeutic resistance. Therefore, characterizing PPIs in AML cells provides critical insights into the functional logic of disease-causing factors. A comprehensive understanding of such interactions not only helps identify critical regulatory nodes but also offers new solutions for the development of therapies aimed at disrupting pathological protein interactions rather than targeting individual molecules involved.

1.2 Protein-Protein Interactions

Proteins are fundamental macromolecules that help maintain biological and chemical balance in the body and they mostly perform their various functions not individually but by interacting with other molecules. This cooperation has important tasks

in living systems as such vital signaling pathways, metabolic events, and cellular processes. The protein-protein interactions (PPI) require high physical specificity. PPI that is formed between multiple protein molecules occurs as a result of various biochemical interactions between the amino acid residues. Hydrogen bonds, hydrophobic interactions and electron-induced electrostatic interactions can be given as examples of that maintain this kind of interaction. PPI disorders are the main cause of many diseases such as cancer, Alzheimer's disease caused by protein misfolding [9]. Investigation of the concept of PPI and targeting different interactions in PPI allows the examination of these biochemical processes and activities [10]. Thus, comprehensive protein interaction networks can be better understood and relevant protein targets can be found for therapeutic purposes.

The proteins in the PPI may be unrelated to each other, in terms of type and structure, but they may undertake different functions within the same large molecule. Thus, small proteins within a large complex molecule can be classified in different ways in terms of PPI. These classifications may be based on signal transduction, membrane transport or muscle contraction functions. In addition, different protein interactions can be observed at different locations during the activity of the molecule. Here, it is important to consider that proteins mostly do this temporarily and sometimes permanently while making these interactions. Thus, complex biological processes can be sustained by the cooperation of separate biological structures. An example of this situation is that in cellular signal transduction processes, most vital activities of the cell are regulated by signals coming from outside or from the cell itself. Protein interactions between various signal molecules ensure that the signal spreads within the cell during this process [10, 11].

Considering all this information, it is clear that the growing interest in PPI in the scientific world can't be denied and the implications to be obtained by a better understanding of PPI give hope for the solution of various health problems [12]. Therefore, it is essential to consider PPI in macromolecules that cause diseases like AML. For this, it is highly necessary to consider the macromolecules that cause the disease and their general structures.

1.3 Kinases

Enzymes are structures that accelerate biochemical reaction rates and regulate various metabolic and biological processes. While performing their functions, they act in a PPI-dependent manner, since they are also proteins. To perform their function, each enzyme has a specific regions to perform their specific function and catalyze their reactions. Enzymes are classified into different types according to their functions, the molecules they interact with, or their structures. They have at least one catalytic domain, and this catalytic domain is the main region where the enzyme catalyzes the chemical reaction. Catalytic domains perform the desired chemical process by bringing together/separating substrate molecules and thus, cellular activities are regulated [13].

Kinase enzymes are a class of enzymes that transfer phosphate groups from ATP molecules to amino acid residues such as tyrosine, threonine, or serine, thereby specifically phosphorylating their specific substrates. The phosphorylation process in question plays a vital regulatory role in numerous cellular pathways, including intracellular signaling, apoptosis, and gene expression. In short, kinases are part of a large and diverse family of enzymes that regulate intracellular signaling networks essential for maintaining cellular homeostasis, in a manner consistent with the principles of PPI [14].

The phosphorylation event occurs on specific amino acid residues and the kinase domain is one of the best characterized and studied types of catalytic domains in the structure of enzymes that specifically performs phosphorylation of the substrates. In addition, some kinase domains are involved in signaling, including cellular processes such as cellular immunity and inflammation [15]. Thus, the kinase domain is also important in terms of interacting with a nucleotide and transferring the phosphate group to substrate proteins [16].

1.4 Tyrosine Kinases

Tyrosine kinases are one type of kinase enzymes and their main function is to transmit signals by transferring phosphate groups to tyrosines on substrate proteins, thus contributing to cellular signal transduction and regulating processes such as cell growth, differentiation and proliferation [17]. Because of these functions, kinases are enzymes

included in the transferase group. As can be seen from Figure 1.1, in kinases, as in other enzymes, there is a specific region for each function, including tyrosine kinases.

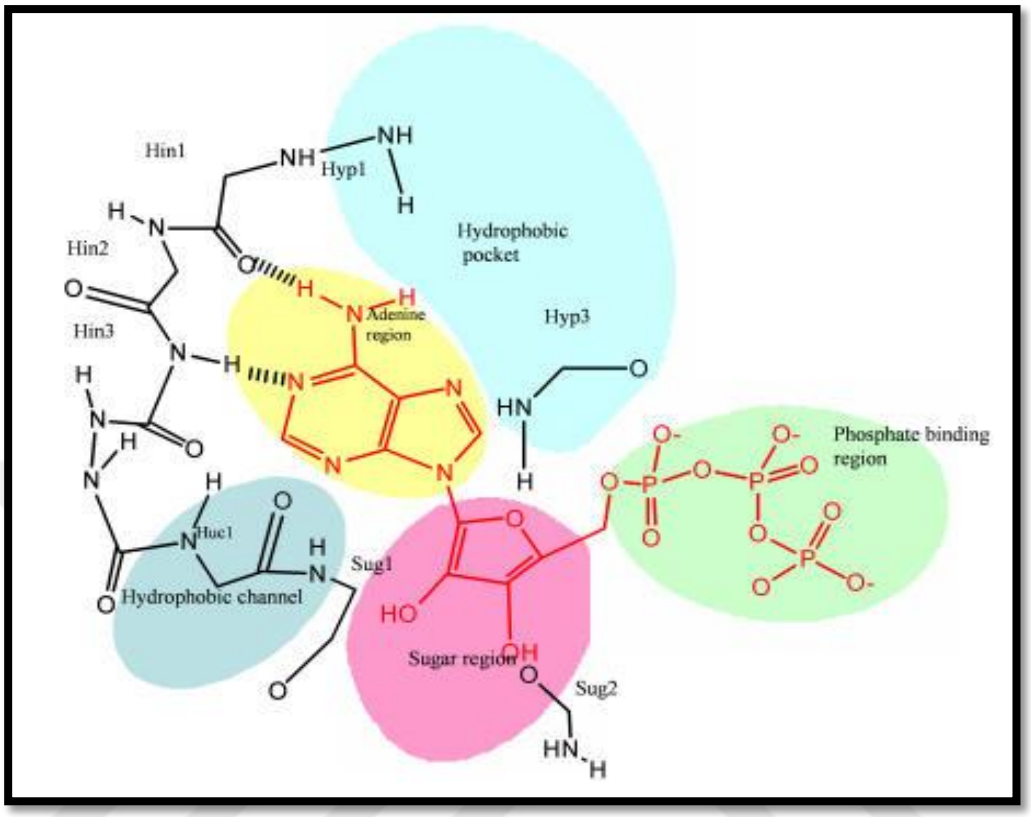

Figure 1.1 Illustration of the ATP binding site of protein kinases (ATP is shown in red) [17].

Tyrosine kinases usually perform their functions in 4 basic steps. During the first step, which is the substrate binding, tyrosine kinase interacts with its target protein; which is called its substrate. This substrate is usually another signal transduction protein. Tyrosine kinase recognizes this substrate through a special binding site. During recognition, auxiliary domains such as “Src Homology 2 (SH2)” mediate the enzyme’s recognition of its substrate. In the next step, which is ATP binding, tyrosine kinase interacts with ATP to transfer its phosphate cluster [18]. Thus, it obtains the phosphate group that it will use in the next step. During the third step, which is tyrosine phosphorylation, tyrosine kinase adds the previously obtained phosphates to specific tyrosine amino acids on the substrate. As a result, the function of the substrate protein changes. In the last step, which is signal transduction, changes resulting from phosphorylation of the substrate initiate or change cellular signal transduction processes.

Initiation/alteration of this signal can trigger cellular responses such as cell proliferation, cell differentiation or cell survival [17].

In conclusion, as its main principle can be seen from Figure 1.2, the phosphorylation process mediated by tyrosine kinase plays an important role in intracellular/intercellular communication. The lack of regulation or excessive activity of tyrosine kinase activity causes uncontrolled growth/proliferation of cells in many diseases, especially cancer. Therefore, tyrosine kinase inhibitors seem promising in preventing uncontrolled cell growth by preventing these conditions, especially in the treatment of disorders [17].

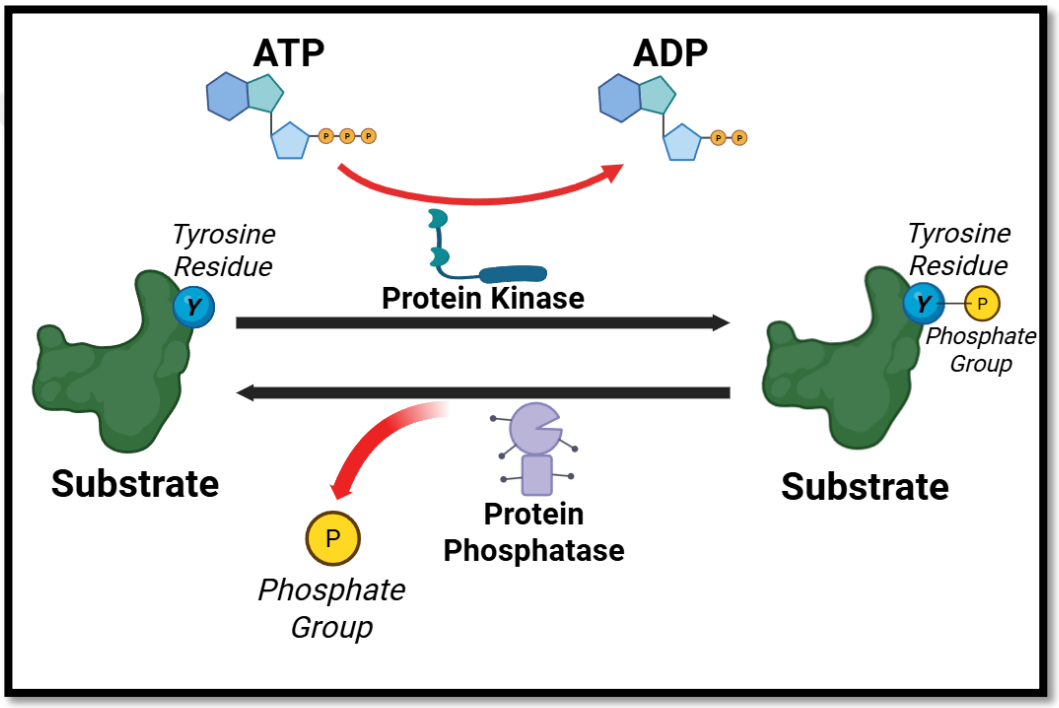

Figure 1.2 Representation of the working principle of tyrosine kinase [19]

1.5 Syk: Structure, Function and Relationship with AML

Syk is a non-receptor tyrosine kinase expressed widely in blood-producing cells. It interacts with receptors containing the Immunoreceptor Tyrosine-based Activation Motif (ITAM) and initiates immune responses through these interactions. It contains two SH2 domains (C-SH2 and N-SH2), two interdomains, and a catalytic domain. As can be seen from the Figure 1.3 [21], it plays a key role in B-cell receptor (BCR) signaling, but its

main effect is in innate immunity via integrins, lectin-like structures, and Fc receptors [20].

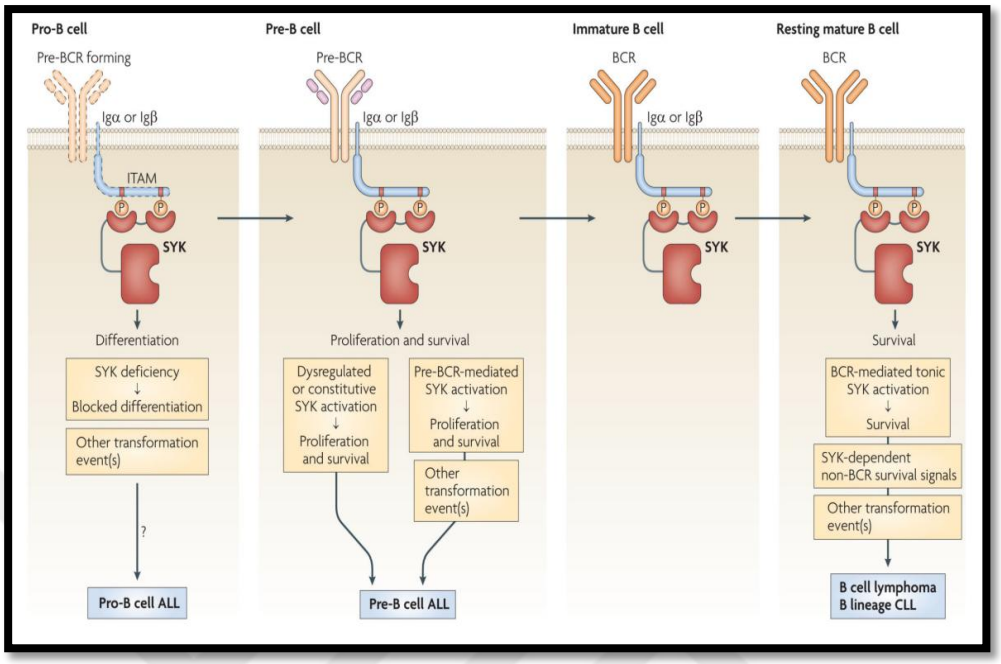

Figure 1.3 Illustration of Syk function in B cell malignancies [21]

Although Syk is also found in tissues other than hematopoietic tissues, it is mostly observed in these tissues and functions in close proximity to the cell membrane. The signals received from B and T immune cell receptors are transmitted to the relevant cell compartments via ZAP70 (Syk cognate) in B and T cells. In addition, Syk activation triggers the activation of "antigen 1" (LFA1), which is associated with the functions of lymphocytes, from the inside out. Thus, the process of "migration", in which leukocytes (white blood cells) leave the bloodstream, begins. As a result, the tight arrest of white blood cells and the activation of the relevant transcriptional changes are achieved [21].

In signaling processes mediated by Syk, in addition to the kinase domain of Syk, the N-terminal SH2 and C-terminal SH2 domains are also crucially important as they mediate the PPI. The interaction between phosphorylated ITAMs and SH2 domains is important for the function of the kinase domain. Phosphorylation of tyrosine residues in the interdomain A and B domains can confer kinase activity even in the absence of phosphorylated ITAMs or ITAM binding [21]. This is due to the ability of the interdomain regions to fold when Syk is inactive. The presence of "constantly active Syk" in cancer also seems to be related to this explanation. Activation of ITAM tyrosine residues through

phosphorylation by SRC family kinases initiates the signaling pathway. Activation is observed after Syk binds to double phosphorylated ITAMs. One group of phosphates binds to the C-terminal SH2 and the other group binds to the N-terminal SH2 (Figure 1.4). This allows Syk to bind directly to binding partners such as PI3K, VAV, and members of the p85α subunit of PLCγ and SLP76 or SLP65 adaptors. These direct binding partners then activate downstream signaling components that trigger various cellular responses such as differentiation, cytoskeletal changes, ROS production, survival and proliferation. An important detail is that other signaling intermediates such as ERK, PYK2 and p38 are also used and participate in these signaling pathways [22].

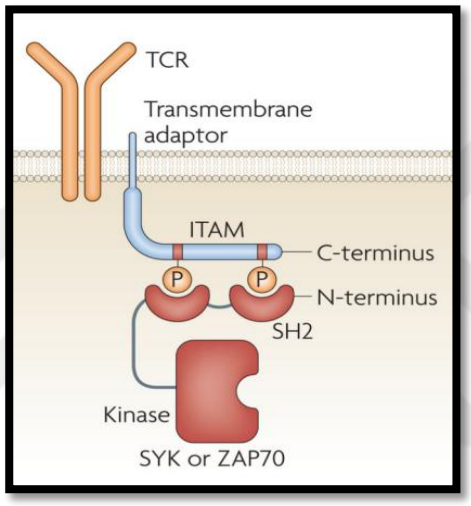

Figure 1.4 Representation of T cell receptor, ITAM and SH2 [21]

As mentioned before, according to studies, Syk enzyme is highly expressed in AML cells and this prevents differentiation. In addition, apoptosis suppression and increased proliferation are encountered [8]. The constant activation of Syk activates intracellular signaling pathways such as NF-κB, JAK/STAT, PI3K/AKT and RAS/MAPK, causing metabolic adaptations and the activation of proteins that prevent apoptosis [8] [23] [24]. Besides, Syk affects interactions with stromal cells in the bone marrow microenvironment. Thus, AML cells can bind to the stroma and this event causes the resistance to chemotherapy [25]. Moreover, epigenetically, Syk can affect DNA methylation, thus suppressing the expression of genes affecting cellular differentiation [21].

Studies on inhibitors such as R406 and entospletinib have shown that targeting the activity of Syk can induce differentiation and apoptosis in AML cells. However, it is clear

that more selective agents are needed due to their specificity limitations [8]. Still similar studies clearly show the importance of the Syk enzyme in the differentiation and apoptosis of AML-related cells. Syk should be considered not only as a kinase enzyme but also as a signaling hub that shapes adaptive survival mechanisms in AML cells. Therefore, reducing or inhibiting the activity of Syk has the potential to collectively block multiple resistance mechanisms in AML cells. Thus, it may be a key target for future approaches such as combination drug use for AML.

1.6 Syk Inhibitors

Considering the information provided and the studies conducted so far, the importance of inhibitors that disrupt the function of the catalytic domain in Syk and directly target it becomes clear. In this context, a selective kinase domain inhibitor that is already used for another purpose can be considered as an important solution candidate. For Syk, the presence of a targetable cavity region that can be seen from the crystal structure of the catalytic domain provides an advantage in terms of finding inhibitors. Binding of an inhibitor that is already known and used for other purposes to the catalytic domain can target specific regions within the catalytic domain and control kinase activity and downstream signaling pathways. This offers strong therapeutic development opportunities in terms of specificity and efficacy. ATP competitive, allosteric, covalent and peptide inhibitors can generally be considered as classes of candidates that can be suggested for the kinase domain of Syk [23].

The most well-known Syk inhibitors compete with ATP binding to the catalytic site, thus blocking the catalytic site. Since these small molecules are mostly structurally very similar to ATP, they form strong interactions with prominent residues in the catalytic cavity. Thus, they prevent ATP binding. Imatinib and R406 are among the ATP competitive inhibitors that have been prominent in clinical studies. As can be seen in Table 1,1, several ATP competitive inhibitors specifically focus on specific residues on the catalytic site of Syk and as a result of these interactions, reduce or completely eliminate the ability of the enzyme to phosphorylate its substrates. Therefore, control of certain responses and functions in cellular signaling is ensured. In particular, R406 has been reported in many studies to bind to the ATP binding pocket of Syk, preventing its kinase activity [20].

Table 1.1 Hydrogen bond analyses of inhibitors interacting with the Syk enzyme. (Abbreviations: hydrogen donor, HD; oxygen acceptor, OA; nitrogen acceptor, NA; Cross-hydrogen bond interactions with the same amino acid are shown in bold.) [26]

H-Bond Interaction								
Ligands	**Pose**	**%**	**H-Bond**	**Ligands Atom**	**Protein Atom**	**Distance (Å)**	**LogP**	**D. M. (Debye)**
Gleevec	1	73	4	N33(NA) O10(OA) N38(NA) H27(HD)	Lys402:HZ1(HD) Ala451:HN(HD) Arg498:HE(HD) Asp512:OD2(OA)	2.217 2.393 2.147 1.995	3.83	5.1101
R406	11	16	3	H9(HD) H25(HD) O36(OA)	Leu377:O(OA) Ala451:O(OA) Ala451:HN(HD)	1.875 **2.262** **2.317**	3.37	3.4870
SykII	1	56	7	H23(HD) H24(HD) O25(OA) H29(HD) H30(HD) H8(HD) H30(HD)	Glu449:O(OA) Glu449:O(OA) Ala451:HN(HD) Arg498:O(OA) Ser511:HG(HD) Asp512:OD2(OA) Asp512:OD2(OA)	**2.075** **2.233** 2.299 2.063 2.558 **2.191** **2.025**	1.22	4.4175
P505-15	8	37	4	H8(HD) O21(OA) H23(HD) H24(HD)	Ala451:O(OA) Ala451:HN(HD) Glu449:O(OA) Glu449:O(OA)	**2.301** **1.888** **1.940** **2.448**	1.02	2.4285

Although Syk inhibitors such as R406 are designed to control the activity of the Syk enzyme and have shown successful results, their effectiveness may face the problem of drug resistance over time. Especially in rapidly spreading, deadly diseases such as cancer, drug resistance is a significant problem and current treatment options may be chronically limited. In the case of drug resistance, problematic cells develop ways to weaken or completely block the effect of inhibitors. These ways include activating additional alternative pathways to the targeted cellular signaling pathways, creating mutations in the regions targeted by the inhibitors, and increasing the pump systems that allow the drugs to remain outside the cell [7].

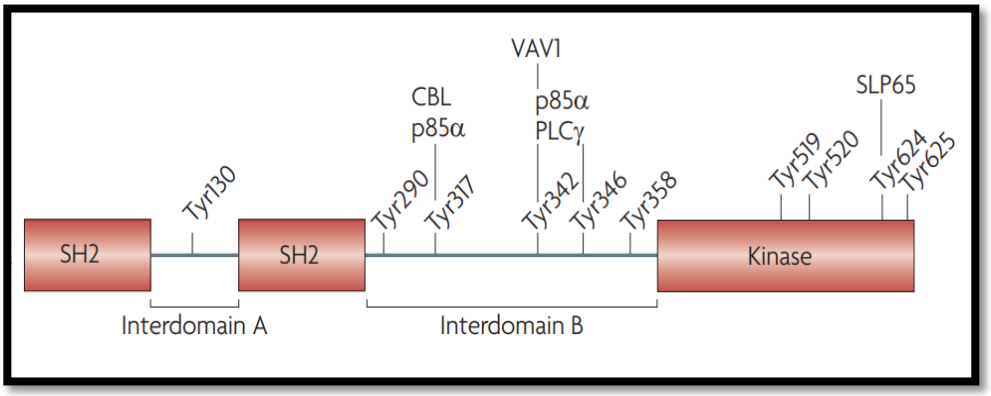

Figure 1.5 Residues indicated as autophosphorylation sites on the Syk structure (Proteins shown to bind to phosphorylated tyrosines are indicated above the tyrosine residues.) [21]

Recent studies have confirmed that BI 1002494 is also a good candidate molecule with high selectivity among Syk inhibitors. It suppresses signal transmission in the relevant intracellular signaling pathways of human basophils at low dose levels (IC50 = ~115 nM), while it shows a therapeutic effect in B cells at relatively higher doses (IC50 = ~810 nM) [27].

Considering all these, it is concluded that more research is needed to increase the effectiveness of inhibitors that work on the catalytic domain of Syk in *in vitro* and *in vivo* studies, by combining them with computer-based molecular docking methods. These studies will lead to the development of effective and safe new solutions in the treatment of Syk-related diseases, especially AML.

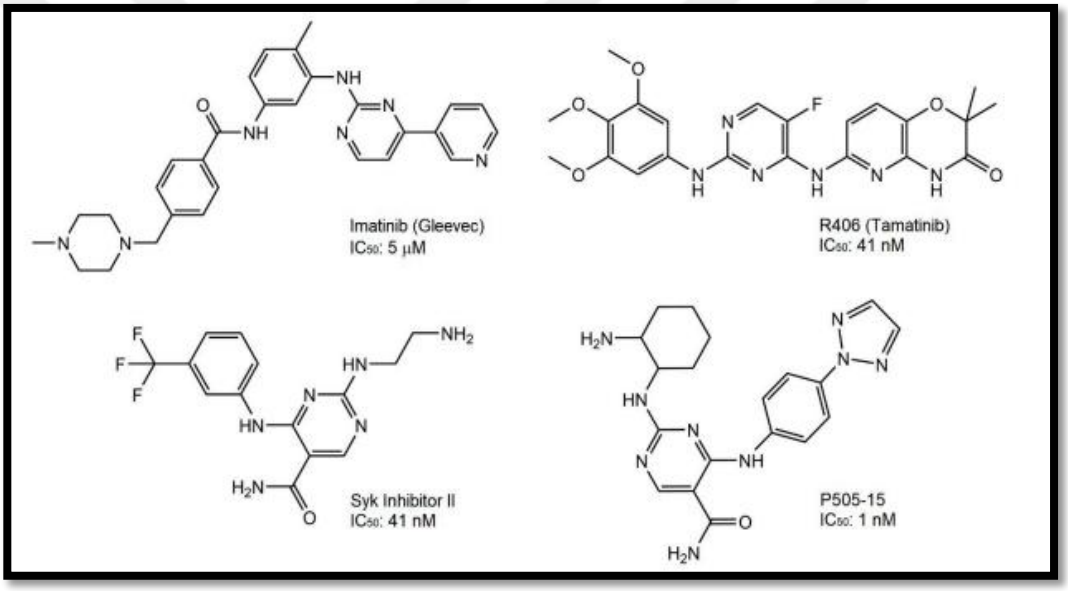

Figure 1.6 Chemical structures and IC50 values of Syk catalytic subunits of Imatinib, R406, Syk inhibitor II and P505-1 [26]

1.7 Molecular Docking and *in silico* Screening Methods

Due to the undeniable role of predicting the interactions between the candidate molecule component (potential drug) and the target protein in current drug development studies, the importance of *in silico* methods has increased today. For instance, in the molecular docking method, the interaction of the focal molecules with the binding pockets in the target molecule is modeled with computer-based tools and the binding energies are

estimated. Thus, many candidate molecules can be removed from the list of the study before the wet lab part, or some molecules can be given priority [28].

Considering the structural features of Syk mentioned above, the catalytic domain with the ATP binding pocket seems to be a logical target for inhibitor binding. For instance, some studies on the design of Syk inhibitors focused on ligand-based pharmacophore modeling, 3D-QSAR and molecular docking analysis, and 99 molecules were evaluated and imidazopyrazine derivatives were shown to have high binding affinity to the Syk active site and good ADME profile [29]. In another study, docking analyses focusing on the binding energies of molecules were conducted via AutoDock Vina, and according to the results, compounds falling below certain molecular binding energies (kcal/mole) were taken into further evaluation [30].

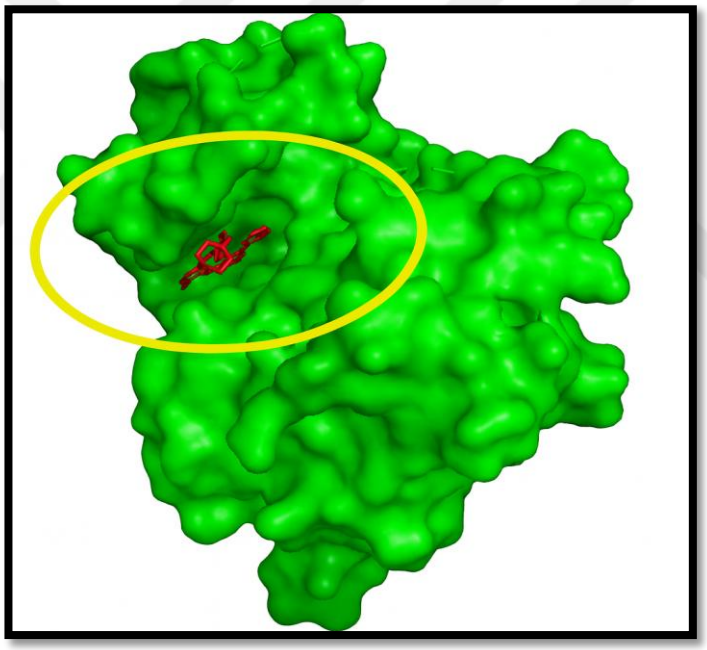

Figure 1.7 *In silico* PyMOL representation of a Gleevec (Imatinib) molecule docked in a suitable cavity (active site) in the catalytic domain of Syk (PDB ID: 1XBB)

As a result, integrating *in silico* methods such as molecular docking with *in vitro* and *in vivo* methods provides a great contribution in terms of saving time and resources. Considering all these, it is understood how important it is to carry candidate molecules identified by *in silico* molecular docking to the biological validation stages. This reveals the importance of *in silico* approaches in drug development studies for prominent targets such as Syk.

1.8 Purpose of the Study

Considering all the information given, this study analyzes the effects of the inhibitor called BI 1002494 (Figure 1.8) [31], which has the potential to suppress the activity of the Syk enzyme, which is a versatile therapeutic target for AML disease, on Syk *in silico* and *in vitro*. BI 1002494 is a novel Syk inhibitor specifically designed by Boehringer Ingelheim in previous studies and obtained using patented synthesis methods in laboratory environment. The molecule's efficacy was studied using enzymatic assays, such as kinase activity assays, and cellular assays, such as basophil/mast cell degranulation, and further confirmed by ex vivo lung studies and *in vivo* models [27]. AML disease is a type of cancer characterized by the uncontrolled proliferation of myeloid cells in the bone marrow, and unfortunately, current treatment methods show insufficient success rates. Syk enzyme is a kinase enzyme that is found in high levels in hematopoietic tissues and plays a key role in intracellular signaling pathways that directly affect differentiation and proliferation. The uncontrolled activation of Syk in AML requires focusing on inhibitors targeting this enzyme.

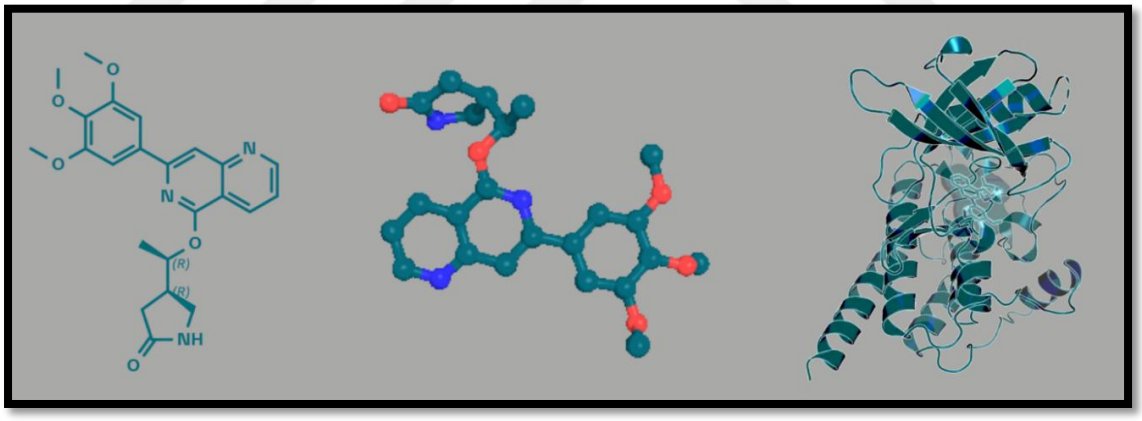

Figure 1.8 2D structure of BI 1002494 (left), 3D structure of BI 1002494 (middle), and BI 1002494 in complex with Syk (right) [31]

In this study, firstly, BI 1002494 molecule was selected which showed high binding affinity to Syk by *in silico* molecular docking experiments performed on candidate inhibitors in opnMe database and a drug repurposing method, which is based on the principle of using existing drugs/inhibitors for the treatment of certain diseases for different diseases, was adopted for Syk enzyme. The catalytic domain and a small part of the “Interdomain B” region of Syk protein were cloned into *Escherichia coli* BL21(DE3)

bacteria using the pET-28a vector. Bacteria were induced with IPTG for an optimized expression level of Syk and recombinant protein production was achieved without any toxic results. The presence and quantity of Syk protein purified by His-tag Ni-NTA affinity chromatography method were confirmed by SDS-PAGE and WB. MOLM-13 and K562 cell lines were used as AML and Chronic Myeloid Leukemia (CML) respectively and cell models in the process and in MTT experiments performed with them, it was seen that BI 1002494 inhibitor suppressed cell proliferation in parallel with the dose and significantly. In conclusion, this study is a new one of comprehensive studies that combines *in silico* and *in vitro* methods to experimentally validate the BI 1002494 molecule as a Syk suppressive inhibitor. The findings and conclusions reveal that the BI 1002494 inhibitor is a valuable candidate for targeted methods in AML disease treatment.

Chapter 2

Materials and Methods

2.1 Study Design and General Approach

In this study, a drug repurposing-like approach was adopted for inhibitor targeting of Syk enzyme. Experiments were performed in three main phases; in the first phase, *in silico* molecular docking analysis was performed for a molecule that is determined to be a candidate molecule as a result of the literature search. In the second phase, recombinant Syk protein production and biochemical validation were achieved. In the third and final phase, *in vitro* biological evaluations were performed in specific AML cell lines. Through this 3-step process, both computational and experimental findings were combined and ultimately, the expected effect of BI 1002494 inhibitor against AML was tested.

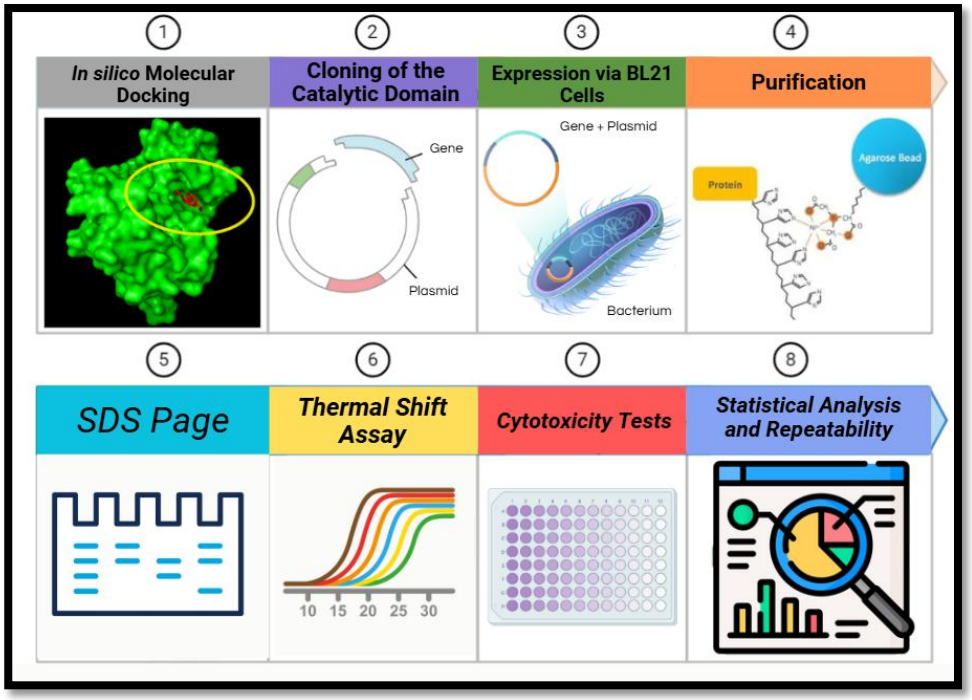

Figure 2.1 Study Design and General Approach

2.2 *In silico* Molecular Docking Analysis

Before proceeding directly to laboratory experiments, a comprehensive literature review was conducted. BI 1002494 molecule, which has been proven to have good metabolic stability, a well-defined production process, is reported to be suitable for *in vivo* studies, and whose negative control (diastereomeric form of BI 1002494, BI-2492) has been reported, was determined as the candidate molecule [32]. During the selection of the molecule, various studies, including some mentioned earlier, considered its ability to be a good Syk-targeting inhibitor for different health problems related to Syk [27] [33]. Furthermore, Besides being ATP-competitive (binding to the active site in the catalytic region of Syk) [27], as the previous studies demonstrated, the molecule's oral availability was another attractive factor in its selection [34].

After the determination of the candidate molecule BI 1002494, *in silico* molecular docking analyses were performed to support the literature review findings for the molecular level interactions of the candidate molecule. First, the virtual and crystal structure of the Syk enzyme (PDB ID: 4FL3) suitable for the *in silico* process was extracted from the Protein Data Bank (PDB) database [35]. Using PyMOL, AutoDock Vina, Discovery Studio Visualizer, and methods from previous studies [30] [36] [37] [38] [39], interactions of inhibitors with known effects such as R406 with Syk were examined on the molecular structure and comparisons were made for interactions with the candidate molecule. It has also been confirmed through literature review that the mentioned methods or similar approaches have been used in different studies for similar purposes [40] [41].

Simulations were performed using the AutoDock Vina software and focused on the ATP binding region of the catalytic domain. The lowest binding energy value and binding poses were recorded for each experiment and then the analyses were visualized with the Discovery Studio Visualizer. According to the analysis results, the inhibitor BI 1002494 obtained from the opnMe database was validated for the laboratory experimental process due to its high binding affinity to the Syk ATP-binding region. The results were also compared with data from *in silico* analyses of R406 and the drug's negative control molecule, BI-2492. Thus, while the candidate molecule was shown to be a reasonable candidate, the reliability of the in silico data was also discussed.

Table 2.1 *In silico* materials, softwares and applications used in the study

Material/Reagent	Description	Process/Step
opnMe	Inhibitor and Candidate Drug Database	*In silico* Molecular Docking Analysis
Protein Data Bank (PDB)	Source of the *In silico* Structures of the Molecules	*In silico* Molecular Docking Analysis
PyMOL	Molecular Visualization Software	*In silico* Molecular Docking Analysis
AutoDock Vina	Virtual Scanning Software for Molecular Docking Simulations, (Version 1.1.2)	*In silico* Molecular Docking Analysis
Discovery Studio Visualizer	Ligand-Protein Interaction Diagrams	*In silico* Molecular Docking Analysis

2.3 Plasmid Construction and Cloning

In the study, the cloning of the targeted entire catalytic kinase domain as well as a portion of the "Interdomain B" region (between residues 356 and 635) was established for the recombinant production of Syk protein, as can be seen from the Figure 2.2. According to the strategy, design of the genetic sequence that will produce the region in question was carried out by SnapGene software starting from the last regions of interdomain B close to the kinase domain and including the kinase domain (between residues 356-635, including those). The aim of the design here was to include some Interdomain B phosphorylation sites such as Tyr358, which is thought to play a role in PPI, protein stability and signal modulation [21] [42] [43] [44] [45] [46]. For this purpose, pET-28a plasmid, which facilitates purification process thanks to its N-terminal 6xHis tag and has T7 promoter (lac operon dependent) and suitable for the bacterial strains to be used in the study, was used from the data and plasmid map taken from the SnapGene [47] [48] [49]. Thus, a total "insert + plasmid" length of 6199 bp was acquired. Since each amino acid is encoded by a three-nucleotide codon, the designed Syk insert is approximately 849 bp long and has the capacity to encode 283 amino acids.

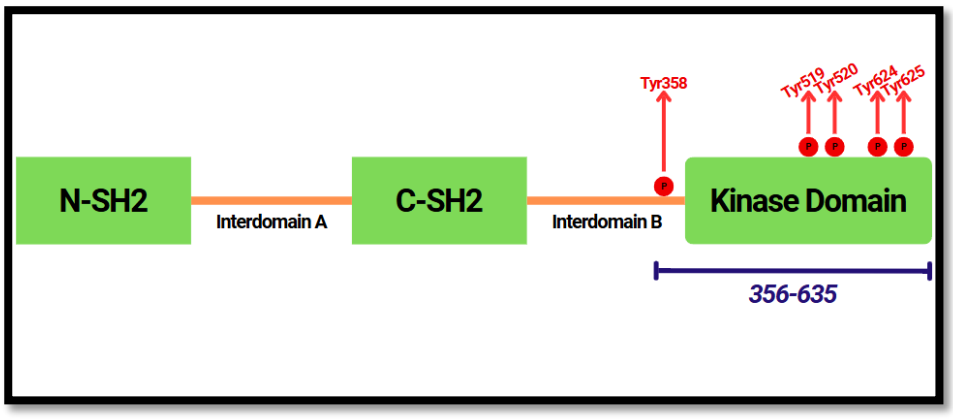

Figure 2.2 Structural diagram showing the N-SH2, C-SH2, Interdomain A/B domains and catalytic kinase domain of Syk enzyme with marked points subject to phosphorylation. The area targeted for recombinant production in the study is also marked separately (between amino acid residues 356-635).

In the study, primers containing EcoRI and HindIII restriction sites were used for the Polymerase Chain Reaction (PCR) amplification step.

- EcoRI (Forward Primer):

5'-GAATTCCATGGAGGAGATCAGGCCCAAGGAGG-3'

- HindIII (Reverse Primer):

5'-AAGCTTGTTCACCCACGTCATAGTAGTAATTCGGC-3'

After the PCR process (95 degrees Celsius denaturation, 69.3/71 degrees Celsius primer annealing, 68 degrees primer extension, 30 repeats) in which different annealing temperatures such as 71 and 69.3 degrees Celsius were tried [50] [51] [52], the concentrations of the PCR products were measured with the NanoDrop 2000 device and it was determined that the most suitable sample was the sample at 69.3 degrees Celsius (30 seconds, 30 repetitions). The process was then continued with this sample.

Then, pET-28a plasmids were transferred to competent *Escherichia coli* DH5-α bacteria (which was grown in Lysogeny Broth (LB) media, 37 degree Celsius with 5% CO_2) for cloning purposes using the "heat shock" method. In the heat shock method, the bacteria were kept on ice at 4°C and then given plasmids (100 microliters of plasmid sample for each 1 ml of bacteria) and subjected to a one-minute heat shock at 42°C. Then, they were immediately put back on ice and the shocking process was completed. Afterwards, the bacteria were left to grow overnight at 37 degrees Celsius in LB agar petri

dishes containing kanamycin. The aim here is to ensure the passage of the plasmid through the cell membrane and if the bacteria acquired the genetic material in the plasmids [53] [54] [55]. The next day, plasmids were obtained in purified form using the NucleoSpin DNA/Protein kit and instructions from bacteria that were confirmed to have accepted and replicated the plasmids through colony formation [56].

After the purification, the "insert" and "vector" ends were cut with EcoRI and HindIII enzymes according to the New England Biolabs' kit and protocol. Then, the "insert + vector" complex was subjected to ligation with T4 DNA ligase in the PCR device at 16°C overnight [57] [58] [59]. The product was cut with the restriction enzymes again and the 5369 bp vector and 849 bp insert bands were directly observed during the agarose gel (50 ml TAE [1X], 0.4 gr agarose, 4 microliters EtBr) electrophoresis process, confirming the success of the ligation process [60].

The obtained recombinant plasmid was transformed and transferred to DH5-α bacteria again by heat shock. Selection was made from colonies grown overnight on selective LB agar plates with kanamycin [61] and these were grown overnight in liquid LB medium containing kanamycin by inoculation. Plasmid isolation was performed with the kit and the presence of the desired recombinant plasmid was proven from the samples run on agarose gel.

The confirmed plasmids were transformed into BL21(DE3) strains suitable for optimum recombinant protein production by the same method. No colonies were formed in the negative control plates as expected for both bacterial strains used in the process (cloning and recombinant production). Antibiotic selectivity in the media was confirmed in this way and the entire cloning process was carried out using methods protocoled in previous studies. Besides the reliability of the results was supported by the Colony PCR method [62] [63].

This construction process enables the combined expression of a protein containing the regulatory/regulated regions and the kinase domain in Interdomain B, thus generating a more comprehensive protein domain for inhibitor binding and phosphorylation assays.

Table 2.2 Plasmid construction materials used in the study

Material/Reagent	Supplier/Brand	Description	Process/Step
pET-28a	Laboratory Stock	Expression Vector	Plasmid Construction and Cloning
Kanamisin	Laboratory Stock	Selective Antibiotic	Plasmid Construction and Cloning
E. coli DH5α	Laboratory Stock	Cloning Bacteria	Plasmid Construction and Cloning
Template DNA (Syk, #6144)	Prof. Dr. Oliver HANTSCHEL's Laboratory Stock	Template DNA for PCR Process	Plasmid Construction and Cloning
Syk Forward Primer	Oligomer Biotechnology	5'-GAATTCATGGAGGAGATCAGGCCCAAGGAGG-3'; Contains EcoRI Cut Site	Plasmid Construction and Cloning
Syk Reverse Primer	Oligomer Biotechnology	5'-AAGCTTGTTCACCCACGTCATAGTAGTAATTCGGC-3'; Contains HindIII Cut Site	Plasmid Construction and Cloning
rCutSmart Buffer	New England Biolabs	Buffers and Enzymes for Restriction Digestion, CAT number: B6004S	Plasmid Construction and Cloning
EcoRI Restriction Enzyme	New England Biolabs	For Cutting from EcoRI Recognition Sites, CAT number: R0101S	Plasmid Construction and Cloning
HindIII Restriction Enzyme	New England Biolabs	For Cutting from HindIII Recognition Sites, CAT number: R0104S	Plasmid Construction and Cloning
T4 DNA Ligase	New England Biolabs	DNA Ligation	Plasmid Construction and Cloning
Taq DNA Polymerase with Standard Taq Buffer	New England Biolabs	PCR Amplification	Plasmid Construction and Cloning
Nuclease-free water	Multicell Sterile Water (Molecular Grade), Wisent Inc.	Sterile, Protease-Free Water for *in vitro* Use, CAT No: 809-115-CI	Plasmid Construction and Cloning
Agarose gel (0.8%)	Laboratory Stock	Gel for DNA Cutting Control, Containing 4 Microliters of EtBr	Plasmid Construction and Cloning

DNA Ladder	Trans2K Plus	DNA Band Size Control Marker, Catalog Number: BM111-01	Plasmid Construction and Cloning
NucleoSpin DNA/Protein kit	MACHEREY-NAGEL	Rapid Isolation of RNA, DNA, Protein and PCR products from the Same Sample (Plasmid Purification and PCR Clean-up, Cat No: 740933.50)	Plasmid Construction and Cloning, PCR Clean-up
NanoDrop 2000 Spectrophotometer	Thermo Fisher Scientific	Quantification Device for DNA, RNA, Protein, Cat No: ND-2000	Plasmid Construction and Cloning

2.4 Recombinant Protein Expression

Escherichia coli BL21(DE3) bacteria, confirmed to carry the Syk insert in the pET-28a plasmid, were grown in LB media containing 50 µg/mL kanamycin at 37°C and under shaking incubation conditions until the optical density (OD in 600 nm) reached approximately 0.65. This bacterial strain was used in the Recombinant Protein Expression stage due to its compatibility with the T7 promoter system, high protein expression yield and low protease activity [64] [65].

Protein expression induction was optimized by adding 0.5 mM IPTG to the culture when the OD value of the culture reached 0.65. After inductions at different temperatures and durations (37°C 4 hours IPTG[-], 37°C 4 hours IPTG[+], 37°C overnight IPTG[-], 37°C overnight IPTG[+], 37°C 4 hours IPTG[+] no plasmid control, 20°C 4 hours IPTG[+], 20°C 4 hours IPTG[-], 20°C overnight IPTG[-] and 20°C overnight IPTG[+]), it was decided that the most appropriate conditions to increase the correct folding of proteins and reduce inclusion body formation were incubation at 37°C for 4 hours [66] [67].

After inducing protein production, bacteria were centrifuged at 5000 x g for 15 min at 4°C and the resulting bacterial pellets were stored at -80°C until purification. Bacteria were lysed with lysis buffer and sonication (10-seconds pulse, 10-seconds pause, 10 minutes in total) to reveal the target proteins inside. The His-tag placed at the N-terminus of the produced protein by plasmid construction was then purified by immobilized metal affinity chromatography (IMAC) containing Ni-NTA resin and explained in detail in the next parts [68] [69] [70].

The expression technique at this stage was implemented based on optimized methods for bacterial recombinant production of tyrosine kinase domains, and the produced recombinant proteins were used for Western Blot (WB) control, Thermal Shift Assay (TSA) and inhibitor binding experiments in the next processes.

Table 2.3 Materials used in the recombinant protein expression process

Material/Reagent	Supplier/Brand	Description	Process/Step
***Escherichia coli* BL21(DE3)**	Laboratory Stock	Protein Expression Bacteria Carrying the T7 RNA Polymerase Gene	Recombinant Protein Expression
Kanamisin	Laboratory Stock	Selective Antibiotic	Plasmid Construction
IPTG	Laboratory Stock	Induction of Protein Expression	Recombinant Protein Expression
T7 Promoter Region	pET-28a Vector	Promoter Recognized by T7 RNA Polymerase	Recombinant Protein Expression
LB Medium	Laboratory Stock	Medium for *Escherichia coli* BL21(DE3) Bacteria	Recombinant Protein Expression

2.5 Protein Purification

The IMAC based His-tag method was preferred for the purification of the obtained recombinant protein. For this purpose, HisPur™ Ni-NTA Superflow Agarose resin and protocol supplied by Thermo Scientific were used. Ni-NTA resin consists of nickel ions (Ni^{2+}) immobilized on agarose beads chelated with nitrilotriacetic acid (NTA). This mixture is used for the high specificity binding of His-tag carrying target proteins. HisPur™ Ni-NTA Superflow Agarose resin has a protein binding capacity of ≥60 mg/mL and works best in the pH range of 3-9 [71].

In the purification step, firstly the resin was incubated with the recommended equilibration buffer (20 mM sodium phosphate, 300 mM sodium chloride, 10 mM imidazole, pH = 7.4). In the second step, the target protein sample and the resin were mixed and binding was ensured (incubation with shaking at +4 degrees overnight after

mixing). Then, the resin and protein mixture was washed with the wash buffer containing 20-30 mM imidazole and the unwanted proteins were removed by centrifugation (700 x g). Then, the elution buffer containing 300 mM imidazole and the samples were mixed and the His-tagged target protein (Syk) in the supernatant obtained by centrifugation was finally purified. The elution and washing steps were repeated twice to ensure complete elution of the protein and 100 microliters of sample were taken for control at each step and stored in separate tubes. The obtained samples were directed to the SDS-PAGE (12%) analysis step for purity control [72] [73].

Table 2.4 Materials used in the protein purification step

Material/Reagent	Supplier/Brand	Description	Process/Step
Ni-NTA Resin Kit	Thermo Scientific, HisPur™	Resin for His-tag Protein Purification, Catalog Number: 88221	Protein Purification
Prime-Step™ Broad Range Protein Ladder	iNtRON Biotechnology	Protein marker used for SDS-PAGE and WB, covering the range of 10–245 kDa, CAT No: 773302	Protein Purification
N-terminal His-tag	pET-28a Vector	6xHis Tag, Used in Purification	Protein Purification
SDS-PAGE Experiment Set-Up	Bio-Rad, Lab Stock	Protein Separation Gel	Protein Purification

2.6 SDS-PAGE for the Protein Purification Validation

SDS-PAGE experiment was performed to verify the purification efficiency of IMAC. Protein samples obtained by purification process were run on gel with 12% polyacrylamide density. Both samples obtained from two consecutive elutions with resin, and also samples taken from each step of purification were tested by placing them in separate wells. In the obtained gel images, remarkable bands around 37 kDa were expected in wells containing purified proteins [74].

In a separate gel, as a control, proteins obtained after IMAC purification from bacteria transformed with empty plasmid (without insert) were also included in the SDS-

PAGE process. In the gel in question, the absence of a band in the elution samples is important in terms of showing that the bacteria with empty plasmid don't produce the relevant protein and don't combine with Ni-NTA resin. The SDS-PAGE results were also supported by the results of the subsequent WB experiment (with Anti-6X His tag) [75].

Table 2.5 Materials used in the SDS-PAGE and WB step

Material/Reagent	Supplier/Brand	Description	Process/Step
Anti-6X Histag Antibody	BioLegend	Purified anti-His tag, Mouse IgG1, CAT No: 652502	SDS-PAGE and WB Analysis
Anti-Mouse Antibody	Laboratory Stock	WB Secondary Antibody (Anti-Mouse)	SDS-PAGE and WB Analysis
WesternBright™ ECL WB Detection Kit	Advansta	WB Protein Detection with HRP-Conjugated Antibodies, CAT No: K-12045-D50	SDS-PAGE and WB Analysis
PVDF Membrane	Immobilon-P Transfer Membrane, Merck Millipore Ltd.	PVDF Transfer Membrane (Pore Size = 0.45 µm) Suitable for WB Protein Transfer, CAT No: IPVH00005	SDS-PAGE and WB Analysis

2.7 Thermal Shift Assay (TSA)

The TSA method was used to analyze the binding stability of the candidate molecule BI 1002494 with the catalytic domain of the Syk enzyme. The TSA method analyzes the change in the thermal melting temperature (T_m) of the target protein as a result of ligand binding. As the hydrophobic regions in the protein's structure become exposed after binding with the ligand, the dye used in TSA binds to these hydrophobic regions, generating a signal. This resulting change in stability is then detected by the qPCR device. Consequently, an inference about binding affinity and T_m can be made based on the data [76] [77].

During the TSA experiment, 20 microliters of the purified recombinant Syk target molecule, whose concentration was measured by Bicinchoninic Acid Assay (BCA) analysis [78] and whose protein structure was confirmed intact by SDS-PAGE (10%),

was added to the experimental master mix (2.5 microliters HEPES, pH 7.5; 2.5 microliters dH_2O; 5 microliters SYPRO Orange, 5X in final; 20 microliters BI 10002494, 10 micromolar in final). BSA and the same protein sample without drug was used, and 50 microliters of solution was completed with dH_2O instead of drug. Additionally, care was taken to ensure that the total DMSO content in the entire solution was below 4%. The resulting 50 microliters of solution was added to special white PCR tubes, placed in the real-time PCR (qPCR) device, and analyzed by adjusting the temperature and measurement parameters specified in the CFX Manager software [79] [80] [81] [82].

First, "File > New > Protocol" path was selected in the main page of the software. Then, in Protocol Editor, "Before" option was selected in the Insert Step dropdown menu and then "Insert Melt Curve" was selected. Then, Delete Step option was selected to remove steps 2-4, leaving only melt curve step 1. Melt Curve range was arranged to 10°C to 95°C in increments of 0.5°C for 10 seconds and "Plate Read" part was added. Sample volume was set to 50 microliters. Then, the plate template was edited in the software according to the samples. From the Scan Mode dropdown menu the "FRET" channel was chosen. Before starting the analysis white plate option was chosen by clicking "Settings > Plate Type > BR White". After about 2 hours, the results were recorded [83].

Table 2.6 Materials used in the TSA

Material/Reagent	Supplier/Brand	Description	Process/Step
SYPRO Orange	Sigma-Aldrich	CAT No: S5692, High Sensitivity Fluorescent Dye for Protein Detection (5000X)	TSA
PCR tubes	NEST (Chemglass)	CAT No: CGN-3610-W-01, 0.2mL white 8-strip PCR tubes, Dnase/Rnase-free, autoclavable, enhances the fluorescence signal in qPCR.	TSA
HEPES (1 M)	Thermo Fisher Scientific	CAT No: 15630080/15630056, ensures pH stability	TSA
qPCR Device	Bio-Rad	96-well real-time PCR Instrument, Provides Precise Data Analysis with CFX Maestro Software	TSA

2.8 Cell Culture

MOLM-13 and K562 cells were grown in RPMI 1640 medium (10% Fetal Bovine Serum [FBS], 1% Pen/Strep) in a 37°C, 5% CO_2 incubator. Routine passages of cells were performed approximately every 2-3 days for both cell lines, and their viability was checked regularly under an inverted microscope throughout the experiment. The inhibitors that have been utilized in this thesis, BI1002494 and BI2494, was kindly provided by Boehringer Ingelheim via its open innovation platform opnMe (available at https://opnme.com) [84] [85].

Table 2.7 Materials used in the cell culturing

Material/Reagent	Supplier/Brand	Description	Process/Step
RPMI 1640 Medium	Gibco	AML Cell Culture Medium, Cat No: 11875093	Cell Culturing
FBS	Gibco	Heat Inactivated Fetal Bovine Serum for Cell Culture Supplementation, CAT No: A5256801	Cell Culturing
K562 Cell Line	Laboratory Stock	Chronic Myeloid Leukemia Cell Line, Low Syk Expression	Cell Culturing
MOLM-13 Cell Line	Laboratory Stock	AML Cell Line Carrying FLT3-ITD Mutation Affecting the Syk Downstream Pathways	Cell Culturing
Pen/Strep	Laboratory Stock	Combination of penicillin and streptomycin antibiotics to prevent bacterial contamination	Cell Culturing

2.9 MTT Cytotoxicity Assays

In cell culture and 3-(4,5-di methyl thiazol-2-yl)-2,5-diphenyltetrazolium bromide (MTT) cytotoxicity assays, human AML cell line MOLM-13 carrying FLT3-ITD mutation and strongly associated with Syk activation was used as the main experimental cell, and CML cell line K562 with less Syk-association than AML cells was used as the control group.

The MTT chemical offers the advantage of being able to determine the viability of cells through the activity of mitochondrial dehydrogenase enzymes. The chemical in question is reduced to formazan crystals due to active mitochondrial enzymes found in living cells. These crystals are purple in color. The purple crystals resulting from the reaction are dissolved and cell viability is determined quantitatively by measuring their absorbance. Thus, values such as IC50 which are important data in drug experiments, are calculated. However, since this enzyme activity is not present in non-living cells, no color change occurs. In other words, no reduction occurs. Thus, quantitative and qualitative comparisons can be made [86].

Drug dose applications were performed on both cell lines. The experimental design was set up with a 96-well plate (each dose with 4 replicates) with a total of 200 microliters of culture (approximately 10 thousand cells) in each well. Drug stock solutions were dissolved in Dimethyl Sulfoxide (DMSO). While cells in the control groups were incubated with only medium, 50 nM DMSO dose was applied to the DMSO control group. BI 1002494 drug applications in the main experimental groups were adjusted at concentrations of 50 nM, 100 nM, 500 nM, 1000 nM, 2000 nM and 5000 nM. The negative control of the drug, BI-2492 molecule, was adjusted to 5000 nM. Cells were grown in the incubator for 48 hours after drug addition. After 48 hours of incubation, 10 microliters of MTT chemical was added to each well and the cells were incubated for another 2 hours. Then, the medium was removed from the wells by centrifugation and 1 ml of DMSO solution was added to each well to dissolve the resulting formazan crystals. After the samples were shaken in the dark for 15 minutes and made homogeneous, the absorbance values were measured at 570 nm [87] [88] [89] [90] [91] [92].

The results obtained from the measurement were analyzed by accepting the control group as standard and the inhibition percentages of the drugs on cell proliferation were determined. The analyses showed that the 2000 nM dose of BI 1002494 reduced the cancer cell viability by approximately half, while the final dose of 5000 nM created a higher inhibitory effect.

Table 2.8 Materials used in the cell culture and MTT cytotoxicity assays

Material/Reagent	Supplier/Brand	Description	Process/Step
MTT	Laboratory Stock	Cytotoxicity Test Reagent	Cell Culture and MTT Cytotoxicity Assays
DMSO	ISOLAB Laborgeräte GmbH	ACS Reagent Grade Used as Solvent in Cell Culture and Molecular Biology Applications, CAT No: 914.036.2500	Cell Culture and MTT Cytotoxicity Assays
Trypan Blue	EcoTech Biotechnology	NutriCulture Trypan Blue 0.4% Cell Viability Dye for Counting Viable vs Dead Cells Under Light Microscopy, CAT No: TRY-B100	Cell Culture and MTT Cytotoxicity Assays

2.10 Statistical Analysis and Repeatability

The experimental data obtained in the study were analyzed in the final form using GraphPad Prism 8 program for statistical analysis. MTT experiments, WB analyses and TSA data were confirmed with at least two independent repeats. In comparing the differences between two groups, $p<0.05$ was considered statistically significant.

The experiments in the study were repeated on different days using optimized protocols and the consistency of the results obtained was ensured. Thus, the reliability and repeatability of the results were ensured.

Table 2.9 Materials used in the statistical analysis and repeatability process

Material/Reagent	Supplier/Brand	Description	Process/Step
GraphPad Prism 8	GraphPad Software	Statistical Analysis Software	Statistical Analysis and Repeatability

Chapter 3

Results and Discussions

3.1 Docking Results and Molecular Interactions

In this section, the binding affinity and interaction of the BI 1002494 with the target protein Syk (PDB ID: 4FL3) were evaluated in comparison with the reference inhibitor R406 and negative control BI-2492. For this evaluation, BI 1002494 were visualized by PyMOL into the ATP binding pocket in the kinase domain of the Syk protein (Figure 3.1). Then, molecular docking analyses were performed using AutoDock Vina. During analysis, a grid box was set to cover the entire binding pocket and the region in question was placed in a way that included the specific amino acid residues of the Syk protein that interact with the ligands. In other words, a suitable area was simulated and visualized that included all the critical points where the ligand could bind.

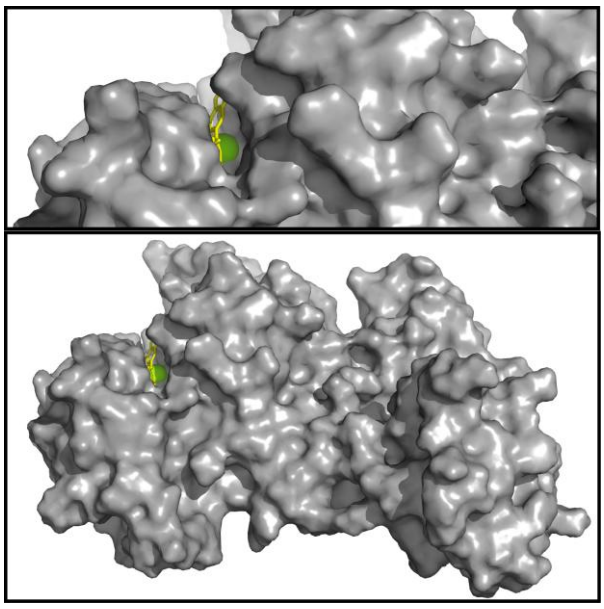

Figure 3.1 Close-up (above) and distant (below) PyMOL visualization of the BI 1002494 molecule in the catalytic domain pocket of Syk protein (4FL3). The green sphere represents Mg^{2+}, which was added to model the ATP/inhibitor binding site as a natural cofactor of kinases in a biologically realistic and electrostatically stable manner.

According to molecular docking carried out by AutoDock Vina software, the binding free energy of the candidate molecule BI 1002494 was calculated as -8.2 kcal/mole. This data shows that the candidate molecule in question binds to the ATP binding pocket of the Syk enzyme in a stable and strong manner. In comparison, the docking score of the FDA approved reference inhibitor R406 is relatively lower (higher binding affinity) with -8.4 kcal/mole, but close to the candidate molecule's scores, which suggests that the candidate molecule BI 1002494 can also form a stable complex with the Syk according to the *in silico* analysis results. These findings can be directly observed from the docking scores and hydrogen bond numbers of both molecules in Table 3.1. The fact that the BI-2492 molecule gave the same binding energy results as BI 1002494 from the blind docking results clearly reveals that the molecule binds to some regions outside the active site (in the computational environment) and that the *in silico* data in question should be interpreted very comprehensively, by including other data, not just by itself alone [93].

Table 3.1 Comparative data on the docking interactions of the candidate molecule BI 1002494 and the reference inhibitor R406 with Syk

Molecule	Docking Score (kcal/mole)	Number of Conventional Hydrogen Bonds
R406	-8.4	3
BI 1002494	-8.2	2
BI-2492	-8.2	2

In addition to AutoDock Vina analyses, *in silico* analyses were also performed with Discovery Studio Visualizer in order to examine the interactions at the molecular level in more detail and comparatively. As can be seen from the Figure 3.2, it is understood that the candidate molecule BI 1002494 establishes "conventional hydrogen bonds" with residues such as Arg498 and Lys458. Besides, it is seen that the candidate molecule establishes "carbon-hydrogen bonds" with some residues like Arg498, Leu377 and Asp512. In the *in silico* findings, different contact points consisting of van der Waals interactions has been also determined between the candidate molecule BI 1002494 and the target protein Syk either. These results are consistent with the fact that the placement conformation in Figure 3.1 clearly shows that the candidate molecule fits into the ATP

binding groove. Comparing with the reference inhibitor R406, the candidate molecule BI 1002494 shows a reasonable conformation either. The molecular shape of the candidate molecule also offer sufficient complementarity with the structural topology of the target molecule, which may be associated with the reasonable docking score of the complex. As a result, the candidate molecule forms direct hydrogen bonds with residues such as Arg498 in silico, as seen in the results of other studies. These inferences increase the reliability of the in silico findings [26] [94].

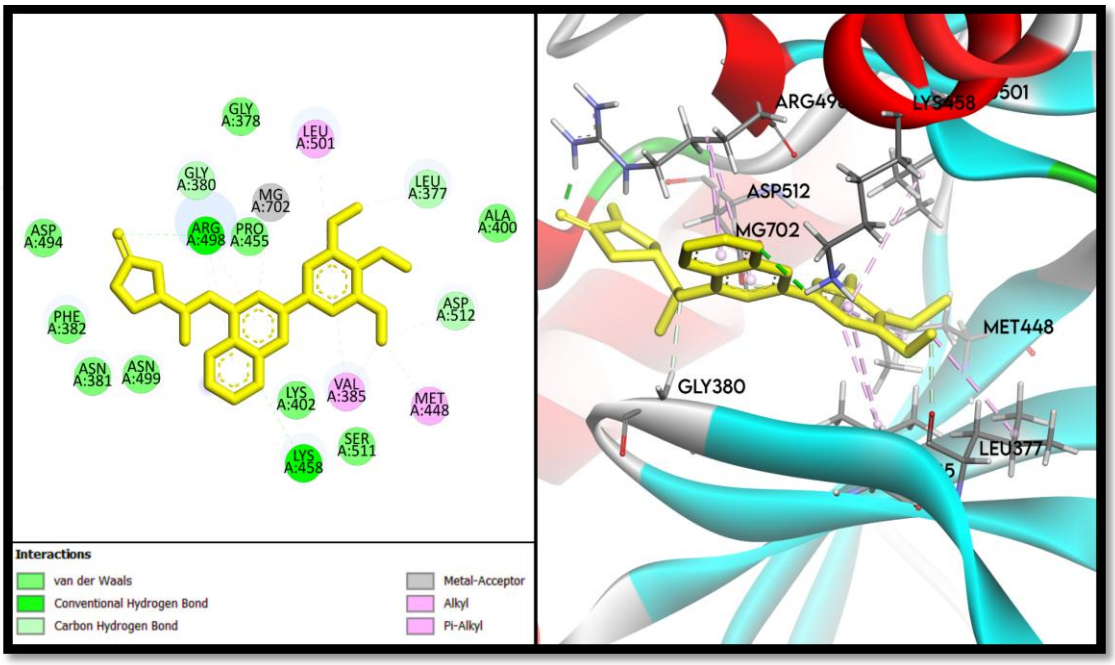

Figure 3.2 2D (left) and 3D (right) interaction diagram of the BI 1002494 inhibitor and Syk protein 4FL3 (taken from the Discovery Studio Visualizer)

These results are consistent with expectations, and as can be understood from the previously given data showing hydrogen bonds formed between Syk inhibitors and Syk, the candidate molecule in the study proves to be a reasonable drug candidate through interactions at the molecular level. Moreover, the results confirm that the candidate molecule establishes a strong molecular interaction with the Syk target protein and is an important inhibitor candidate that can be used for *in vitro* and *in vivo* experiments. The fact that this *in silico* pre-selection step has been used in different studies, just like in this study, increases the reliability of the findings.

3.2 Recombinant Protein Expression and Purification

In this section, the target protein was produced by recombinant ways for use in inhibitor tests and biochemical analyses. The production in question was made using the BL21(DE3) strain of *Escherichia coli* bacteria, which is preferred in scientific research and provides optimum expression. The gene region studied was first inserted into the pET-28a vector with a His-tag and then transferred to the target host bacteria through the transformation process, as can be seen from the Figure 3.3.

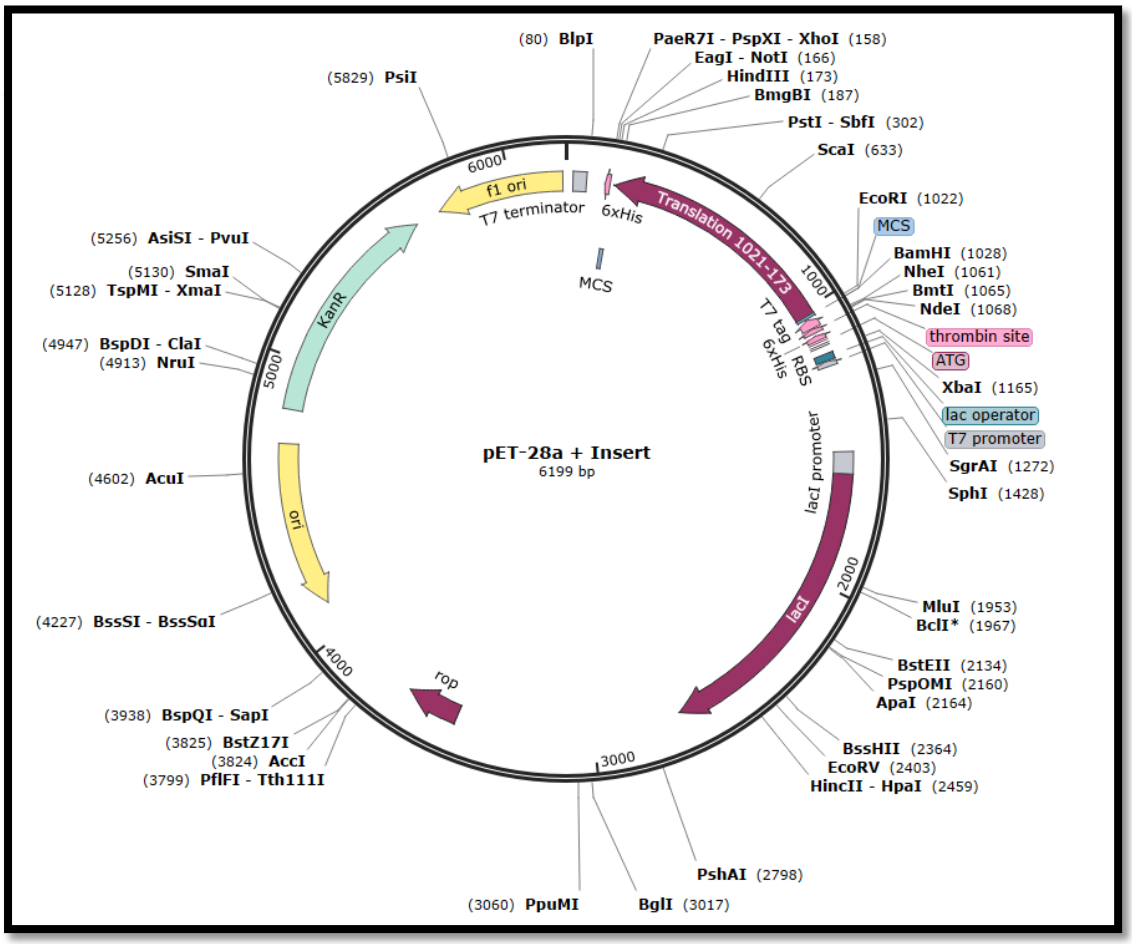

Figure 3.3 Map structure of the "pET-28 + Insert" design used in the study (taken from the SnapGene software)

After the transformation, in case some bacterial colonies (for both DH5α and BL21 strains) were able to grow despite the ligation failure [95], the presence of the target recombinant DNA was reported multiple times by processes such as growth in selective liquid media containing antibiotics, colony PCR (Figure 3.4), agarose gel running (Figure

3.5) and protein purification after culturing. Thus, bacterial colonies grown in LB agar media containing antibiotics were reported as representing the recombinant bacteria obtained after successful cloning, ligation and transformation (Figure 3.6). Additionally, studies have indicated that improvements can be made in preventing false positive colonies for high-quantity production using some methods [96].

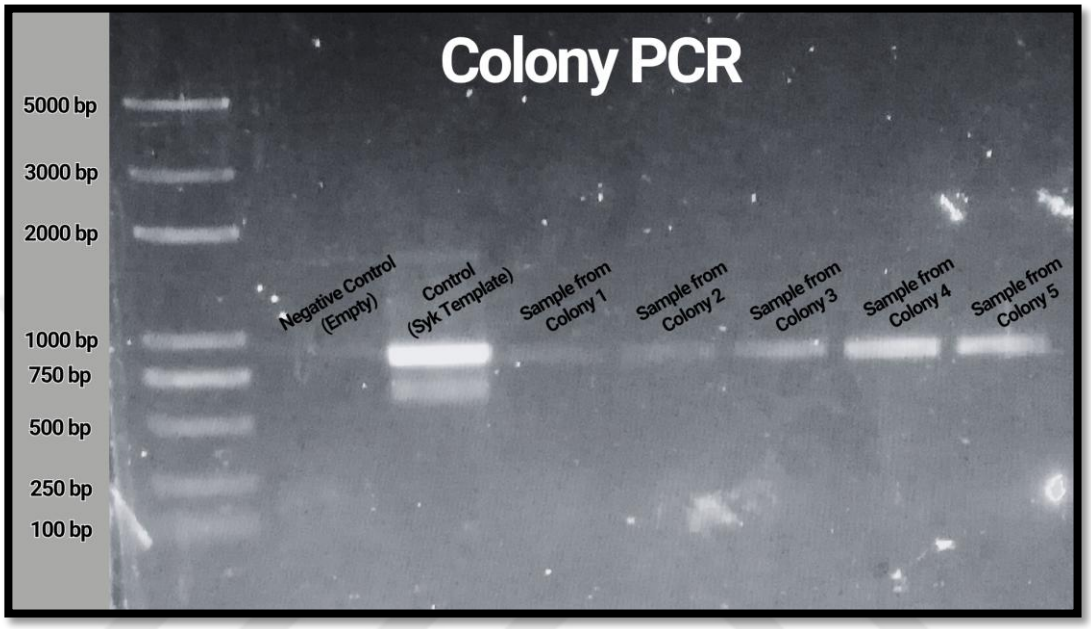

Figure 3.4 Colony PCR results from different colony samples of transformed DH5α bacteria

As seen from the results of the colony PCR experiment, bands were not observed in some colonies due to the lack or absence of DNA sequence to express the target protein. This situation shows the importance of verifying processes such as ligation in more than one way. There may be many reasons for colonies growing despite unsuccessful ligation. One of these is insufficient contact with the selective antibiotic in the medium. Against such possibilities, the importance of verifying ligation with colony PCR and methods after plasmid isolation has thus been revealed.

As can be seen from Figure 3.5, colony PCR results were supported by cutting the plasmid with HindIII and EcoRI enzymes. Since the cutting process or the cutting enzyme activity may be insufficient in some cases, it is possible to see the uncut bands in the agarose gel. However, the fact that the samples that were cut were very small and that the cut and uncut bands could be clearly distinguished increases the reliability of the findings. Moreover, it is thought that the “PCR Clean-up” stage is essential for a more reliable

ligation. As stated in previous studies [97], it can be said that residues and chemicals from the previous processes performed before ligation may affect ligation success, and therefore methods such as PCR Clean-up should be optimized and applied carefully. The failure of some ligation experiments that were tried to be carried out without PCR Clean-up in the experiments supports this idea.

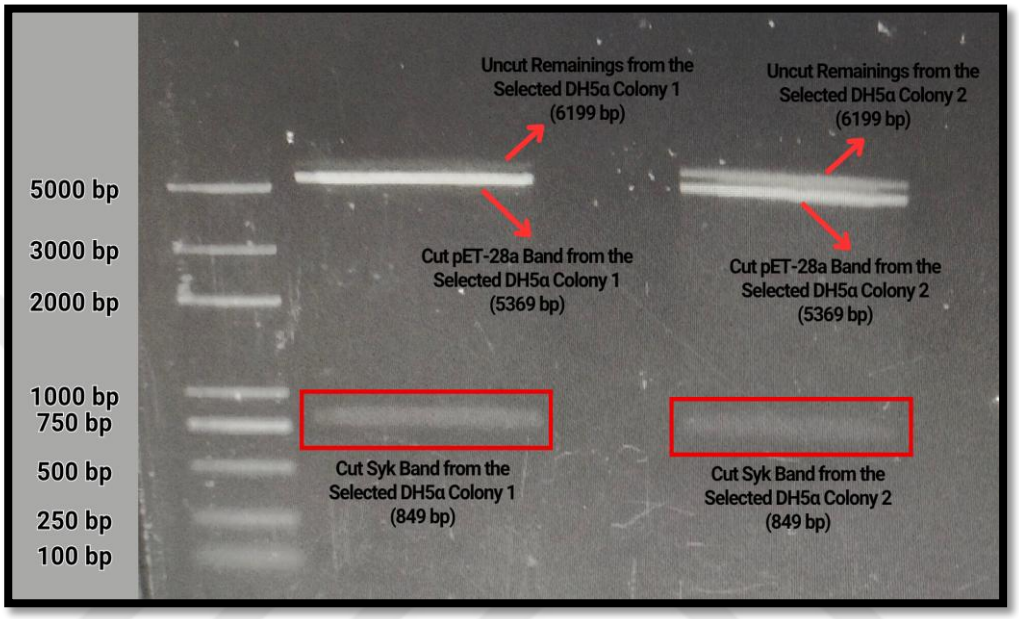

Figure 3.5 Agarose gel running results of the restriction enzyme cutting after the ligation of Syk insert and pET28a vector

Figure 3.6 BL21 bacterial colonies carrying target recombinant DNA after transformation

Samples selected from BL21 colonies were inoculated and the expression process was started again by re-culture in liquid medium. IPTG addition was made as 0.5 mM when the bacteria reached 0.65 OD concentration value (50 microliters of IPTG with a concentration of 0.5 M to 50 mL bacterial culture). During IPTG induction, different induction conditions were tried to determine which condition was best in high-quantity production process. According to SDS-PAGE gel running results, it was determined that IPTG induction for 4 hours at 37 degrees Celsius was the best condition (Figure 3.7), consistent with the data from the literature and the material providers [64] [98]. Furthermore, studies have indicated that the recombinant production of some unstable proteins can lead to destruction by factors such as proteases during long-term production, and that protein amounts can be lower than during short-term production. This may indicate that the recombinant protein produced in this study is unstable since it only contains the active site and a part from the Interdomain B. Thus, these findings could also explain the protein decrease observed during overnight production. [99] [100]. To prevent these problems, using lower doses of IPTG may also be considered.

In WB results, recombinant Syk traces were observed in some samples that weren't given IPTG due to "leaky expression" or leaks that may have occurred to the side wells during loading (Figure 3.8). It has been stated in different studies that the reason for this situation may be a defect in the T7 promoter region used in this study, and the use of different types of plasmids has been suggested to avoid this situation [101] [102]. In addition, when the molecular weight of the produced Syk was calculated by taking into account the length of the coding DNA sequence (~849 bp) and the added vector regions, it was observed in the results that the band lengths were in the expected regions (Figure 3.7). In this calculation, the average molecular weight of the amino acids was taken as 110 Daltons. According to the calculation of "849 bp / 3 = 283", a molecular weight value of approximately 31.1 kDa was calculated for the insert part of the protein over 283 amino acids. In addition, when the N-terminal His-tag and linker sequences (~25 amino acids) from pET-28a are also taken into account, an additional 2 kDa molecular weight emerges. When all these analyzes are taken into account, the molecular weight of the protein to be produced in total was predicted as ~33 kDa. This molecular weight is also consistent with the bands observed in SDS-PAGE analyzes and confirms that the recombinant protein was successfully produced. As expected, no band was observed in the bacterial control

group samples carrying empty vector and placed in the WB assay to verify the specificity of expression.

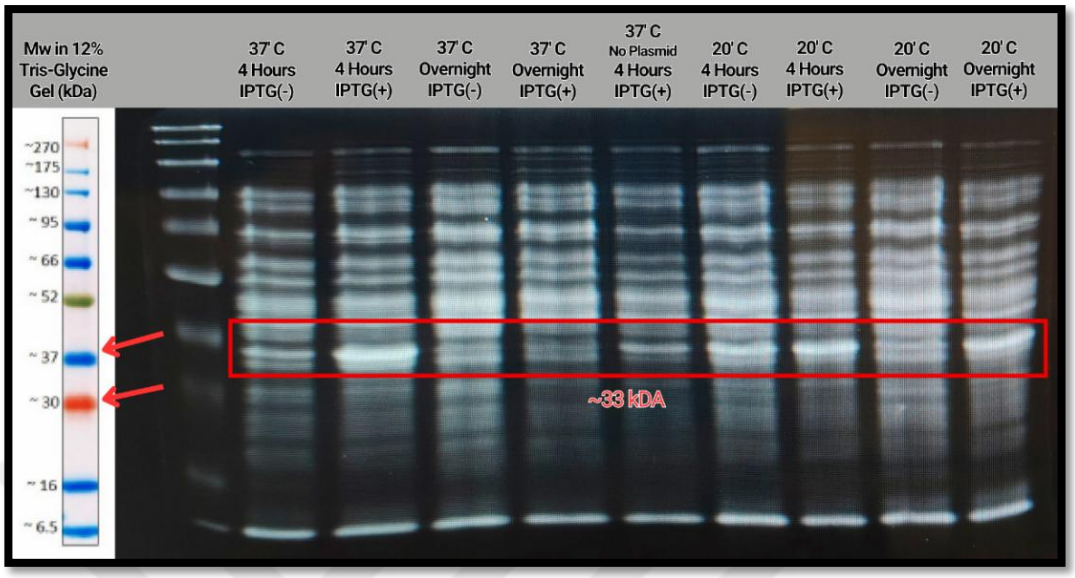

Figure 3.7 SDS-PAGE results of the optimization experiment performed at different temperatures and times for IPTG induction

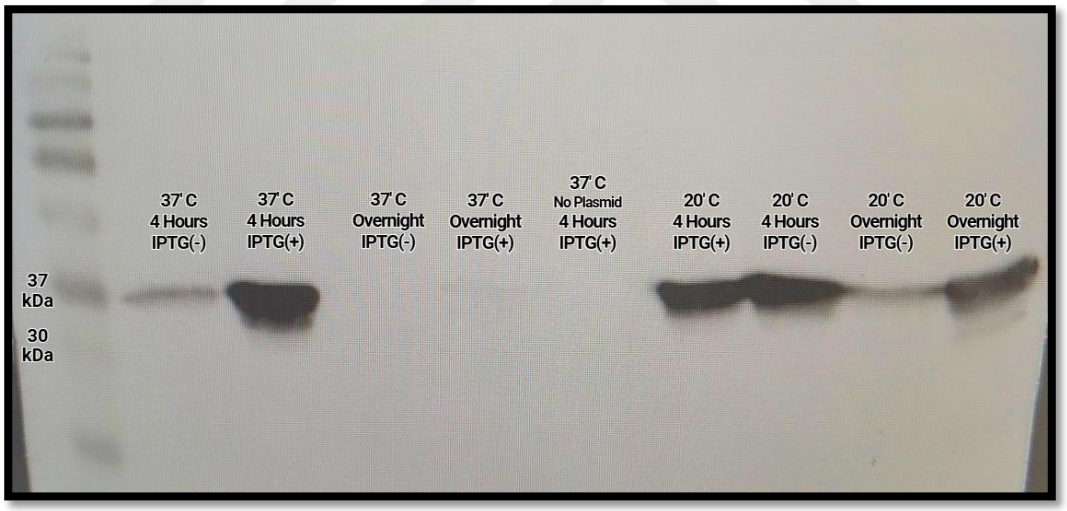

Figure 3.8 Possible "leaky expression" bands have been observed in samples without IPTG in anti-His WB analysis. Yet, the overall results show the success of the recombinant protein production.

After determining the optimum conditions, the large-scale production phase was started and proteins were harvested from 800 mL bacterial culture grown for 4 hours at 37 degrees Celsius with 50 mM IPTG. Purification of the target protein was carried out using the IMAC method, focusing on the 6xHis-tag added to the N-terminal part. As a result of the analysis with SDS-PAGE, where samples taken at each step of the

purification were used, it was understood that the elution samples made 2 times in a row were obtained with high purity. In addition, the fact that no protein band was observed in the WB results at the end of the purification process with proteins harvested from bacteria with empty plasmids used as controls was another evidence proving the specificity of expression. However, the interpretation of the faint bands seen in the region close to 33 kDa of empty plasmid samples was left to the future studies (Figure 3.9 and Figure 3.10). Moreover, these results are consistent with those shown in previous studies, and although toxic effects may be observed in some cases, they show that production of Syk protein alone at high concentrations, even as only the catalytic domain, does not harm the recombinant production systems and is compatible with those used in the study [103] [104].

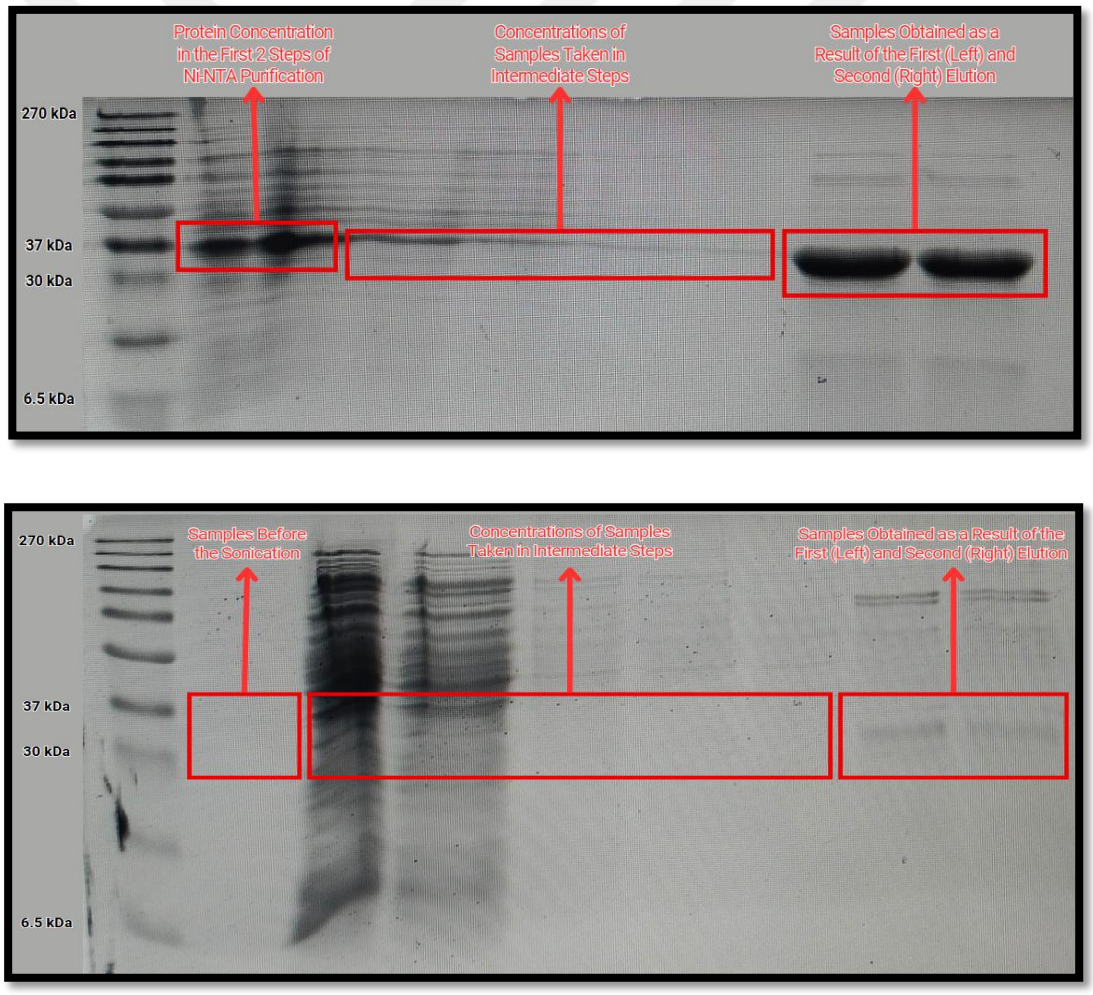

Figure 3.9 and 3.10 Ni-NTA resin purification results of the samples (above) and the control group (empty plasmid, below)

These findings show that the protein can be successfully produced recombinantly and that the production doesn't have a direct toxic effect on the cell at all steps. On the other hand, the fact that the WB band intensities were lower at all temperatures in long-term recombinant production experiments such as overnight growth compared to short-term ones (including the faint band at 37 degrees Celsius, overnight incubation) also suggested that long-term production may have a direct or indirect effect on the degradation of the proteins in question. The fact that no protein traces were found in the samples with empty plasmids and that the recombinant protein was produced as desired after purification demonstrated the reliability of the recombinant production process of Syk with pET-28a plasmid in BL21 bacteria.

3.3 Analysis of Ligand Binding Stability by TSA

The TSA experiment was conducted to analyze the thermal stability changes resulting from the interaction of the recombinantly produced target Syk protein with the inhibitor BI 1002494. This method is a biophysical assay that analyzes protein-ligand binding through the increase in T_m observed due to the ligand's stabilization of the protein's three-dimensional structure. In this study, the SYPRO Orange dye, known to fluoresce due to the opening of hydrophobic regions resulting from molecular changes caused by ligand-protein interactions, was used.

To analyze whether the recombinant Syk target protein, purified by Ni-NTA affinity chromatography, retained its desired protein structure before treatment with SYPRO Orange dye due to the delay, the presence of the protein was reconfirmed by SDS-PAGE. The results revealed a protein structure even purer and more stable than that of the BSA control (Figure 3.11). BSA was used as a control here since, as seen in previous studies, the arrangement of the multiple disulfide bonds in BSA plays a decisive role in the folding and stability of the protein. Therefore, it maintains its structure for extended periods and can be used as a control in experiments like TSA, given that its structure remains intact [105] [106]. The candidate molecule BI 1002494 was included in the assay at a concentration of 10,000 nM, which correlated with the values in the MTT cytotoxicity assays. An equivalent volume of purified water was added instead of inhibitor in the control groups. Thus, in order to prevent DMSO from affecting the SYPRO Orange study, DMSO rates were kept below 4% in total volume.

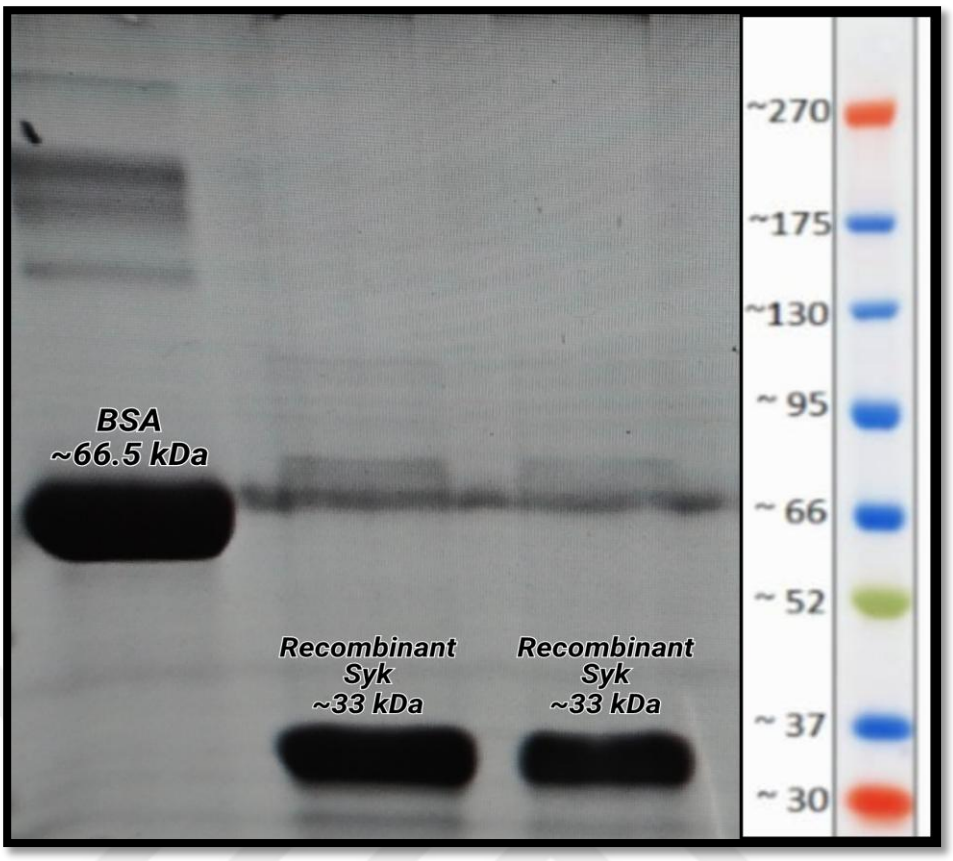

Figure 3.11 SDS-PAGE (10%) results of the recombinant protein before TSA compared with the BSA protein as control.

Each reaction mixture/assay was prepared in triplicate in white qPCR tubes, and the data were analyzed in separate experiments. SYPRO Orange dye was added to the PCR tubes last. TSA analyses were performed using a Bio-Rad qPCR instrument compatible with CFX Manager, taking fluorescence measurements at every 0.5°C increment from 5°C to 95°C. Although buzzy fluctuations and excessive signals were observed in the data obtained from samples other than BSA, which were used as controls, significant data were reported when Tm values were calculated from the first derivative inflection points of the melting curve (Figures 3.15, 3.16, and 3.17). As a result of the experiment, it was reported that Tm values in samples containing BI 1002494 were significantly increased compared to the control groups in all experimental replicates. While the average Tm value was measured as 61.5°C in the control group, this value was measured as 74°C in the 10,000 nM BI 1002494 group. BSA, used as control, showed an average Tm of 64°C, consistent with literature values [107]. The approximately +15°C increase observed with BI 1002494 demonstrated dose-dependent binding stabilization by the inhibitor.

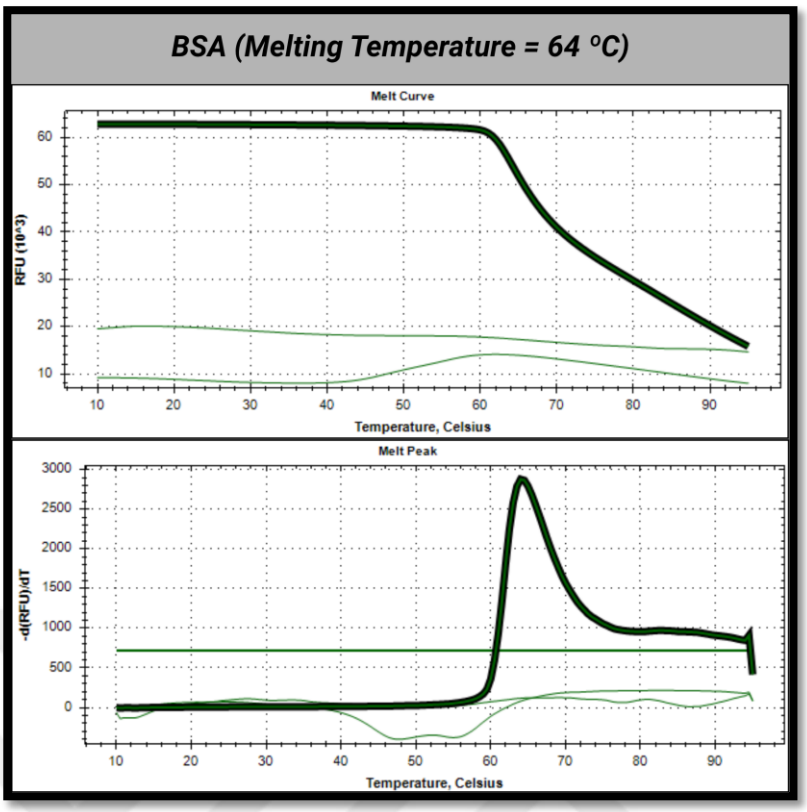

Figure 3.12 Melt Curve and Melt Peak results obtained from the TSA experiment of the control BSA protein

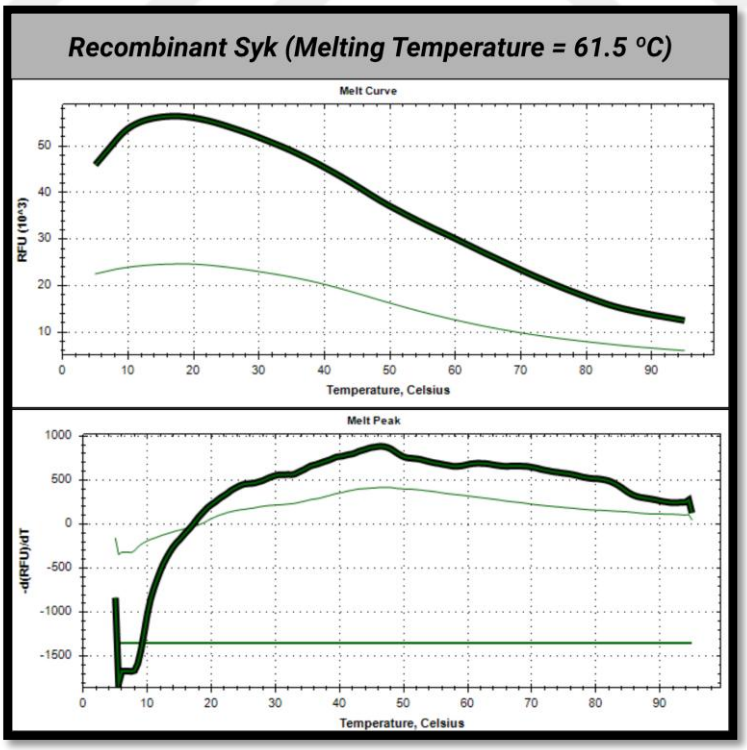

Figure 3.13 Melt Curve and Melt Peak results obtained from the TSA experiment of the recombinant Syk protein

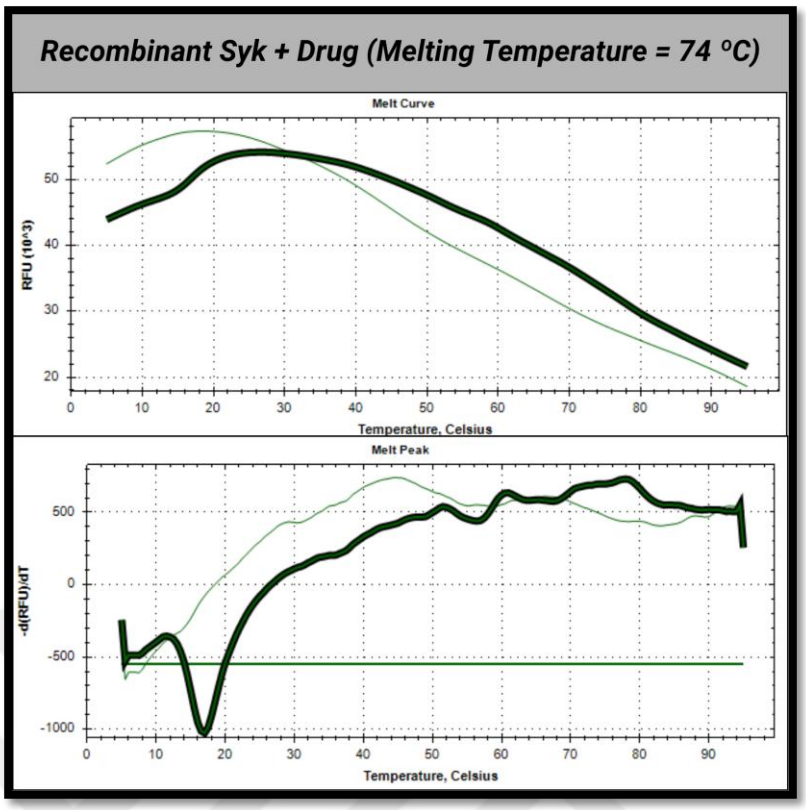

Figure 3.14 Melt Curve and Melt Peak results obtained from the TSA experiment of the "Syk + Drug" complex

The buzzing fluctuations and excessive signaling observed in samples containing Syk protein during the TSA process were considered based on the results. It was suggested that this might be due to the recombinant production of only a specific portion of the protein, rather than the entire protein. The literature indicates that some alternative forms, such as a point mutation at Tyr-348, can lead to destabilization even in the inactive form of the protein (and that this region is missing in the recombinant protein), which was considered a clue to explain this situation [42] [43] [44] [45] [46]. On the other hand, some studies have shown that mutations at specific phosphorylation sites, despite occurring, cause minimal changes in TSA results. Therefore, it has been inferred that the excessive signals in the graph are due to the "absence" of interdomains and SH2 domains, which are thought to be directly involved in the Syk stabilization [118]. Moreover, previous studies have reported that even in the absence of protein, when the dye and buffer solution mixture is not chilled, artificial signals resembling a "melting curve" may be formed [82], and noisy or unexpected curve shapes may appear on the graph due to protein instabilities such as partial unfolding/aggregation [109].

These results support the results of *in silico* docking analyses showing that the candidate molecule BI 1002494 binds with high affinity to the ATP-binding site of the Syk protein. This suggests that the molecule's stability increases when combined with the target protein, suggesting that the molecule could be a strong candidate for Syk-targeted AML therapies.

3.4 Cytotoxicity Assays and IC50 Analysis

In this section, the effects of different doses of the BI 1002494 inhibitor on AML cell viability through Syk inhibition were discussed with the MTT cytotoxicity test. Since this test is based on the logic that the mitochondrial activity of the cell provides information about the metabolic status of the cell, it was used to determine the cytotoxic effects of the candidate drug. In addition, the BI-2492 molecule, which is the negative control of the inhibitor, was also included in the experiments. Experiments were performed on the AML model cell lines MOLM-13 (high expression level of Syk) and the other one used as a control, K562 (minimally affected by the inhibition of Syk) [110]. Both cell groups were grown for 48 hours with BI 1002494 and BI-2492 at the previously specified concentrations. Then, MTT chemical was added to the cells and the cells were incubated for 2 hours. The formed formazan crystals were dissolved and their absorbance values were measured at a wavelength of 570 nm.

In the results of the experiment on the MOLM-13 cell model with the candidate molecule BI 1002494 at drug doses of 50 nM, 100 nM, 500 nM, 1000 nM, 2000 nM and 5000 nM, viability was above 90% at low doses between 50 nM and 500 nM, while significant decreases were observed in viability rates starting from the 1000 nM drug dose. Cell proliferation values were reported below 50% at doses of 2000 nM and 5000 nM, and statistical significance was reported at the level of "$p < 0.0001$ (***)" at these doses. The negative control drug BI-2492 revealed interesting cytotoxicity results in MOLM-13 cells. Although it didn't have an effect on cell proliferation as it should have in the first experiment, it was observed that the molecule had a negative effect on cell proliferation in the second and third repetitions. This situation led to the emergence of a statistical result such as "$p < 0.01$ (**)". The results of the control and DMSO groups didn't have a significant negative effect on cell proliferation as expected.

In the results of the assays performed with the candidate molecule BI 1002494 in the control group K562 cell line, cell viability was reported as high at all doses as expected at the previously mentioned drug doses. It was observed that cell proliferation levels were negatively affected only at drug doses of 1000 nM and above, and even at the highest dose of 5000 nM, viability rates were at 80%. The values in question were found to be statistically significant at the level of "$p < 0.05$ (*)", but didn't reach cytotoxic levels as desired. Here, the negative control molecule BI-2492, tested at a dose of 5000 nM, didn't show a significant cytotoxic effect on cell proliferation in the experimental repetitions ($p < 0.01$ [**]). The data in question is consistent with the negative control feature of BI-2492. In the DMSO groups, K562 viability didn't show a significant decrease as expected, and the reliability of the experimental setups was supported. As a result, when three different experimental replicates were considered, no significant proliferation decrease was observed in the K562 cell line due to drug doses. It was also determined that the variation between experiments was minimal.

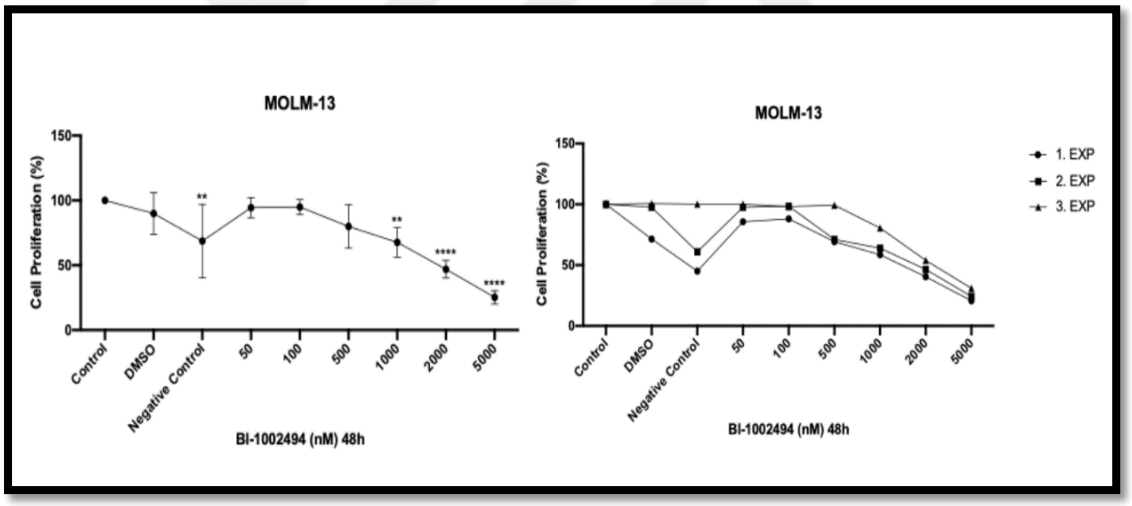

Figure 3.15 Effects of BI 1002494 and BI-2492 at different doses on proliferation in MOLM-13 cells at 48 hours (On the left, average of all experiments; on the right, separate results of 3 repetitions).

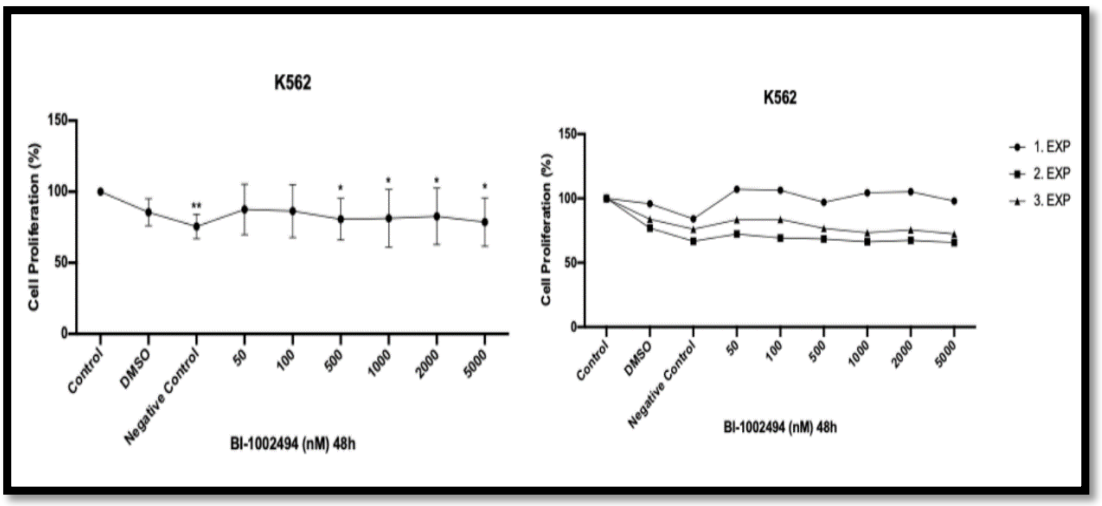

Figure 3.16 Effects of BI 1002494 and BI-2492 at different doses on proliferation in K562 cells at 48 hours (On the left, average of all experiments; on the right, separate results of 3 repetitions).

Evaluation of the data obtained from the MTT assay using non-linear regression (log(inhibitor) vs. response – variable slope) analysis in GraphPad software showed that the IC values for the BI 1002494 molecule for the MOLM-13 cell line were 239.6 nM (IC10), 411.3 nM (IC20), 588.9 nM (IC30) and 1036 nM (IC50), respectively. As previously mentioned, the IC50 value reported from enzyme assays for R406 in the literature is reported as 41 nM [26]. This reveals that the R406 inhibitor has a ~25-fold higher potency than the BI 1002494 candidate molecule. Due to the pharmacokinetic properties of the BI 1002494 candidate molecule, which should be compared separately with R406, it shouldn't be ignored that its utility *in vivo* may be close to or even superior to the R406 molecule. Therefore, considering that the BI 1002494 inhibitor hasn't been directly tested against AML in the literature, it has also been inferred that it has an important novelty value in terms of evaluating new structural combinations. Thus, comments on the need for comprehensive future investigation of the inhibitor's efficacy, supported by pharmacokinetic and pharmacodynamic data, are left to the future prospects section. As a result, these findings revealed that the BI 1002494 candidate molecule had a parallel effect with increasing doses in the MOLM-13 cell line and showed a reasonable inhibitory effect, just like in the similar previous studies [8] [111].

Table 3.2 Calculated Inhibitory Concentration (IC) / values for BI 1002494 inhibitor in MOLM-13 cells

IC / Inhibition Level (%)	Concentration (nM)
IC10	239.6
IC20	411.3
IC30	588.9
IC50	1036

These findings demonstrated the cytotoxic effects of the candidate molecule BI 1002494 on MOLM-13 and K562 cells with MTT assay data. The MTT findings in question are particularly valuable because they bring all these points together in this study. Consistent with the dose increase in the AML cell model, significant proliferation inhibition was detected, especially at 2000 nM and 5000 nM drug doses. At high doses, cell viability decreased below 50% as expected and statistical significance was demonstrated at the "$p < 0.0001$ (****)" level. As expected (although variable across repetitions), the negative control of the candidate molecule, BI-2492 molecule, didn't cause significant cytotoxicity in MOLM-13 cells as expected. In the K562 cell line, the viability rates of the candidate molecule were at high levels (80%) at all applied doses, and noticeable decreases ($p < 0.05$) were detected only at high doses (≥1000 nM). The IC50 value, which is one of the focal points of the findings, was determined as 1036 nM for the MOLM-13 cell line. All the findings in question revealed that the BI 1002494 candidate molecule had a strong inhibitory effect on AML and didn't create any significant cytotoxicity in K562 cells, which represent non-AML cells.

3.5 General Statistical Evaluation

The analysis of all data and findings obtained in the experiments were performed statistically using GraphPad Prism 8. The data and findings in question were obtained with three experimental repetitions and the means and standard deviations were taken into account when evaluating the results. In all analyses, the value of "$p < 0.05$ (*)" was considered statistically significant. Moreover, the repeatability of all experiments and assays was high and the coefficients of variation were evaluated within acceptable limits.

3.6 General Discussion of the Results

This study followed a path encompassing scientific methods such as *in silico* molecular docking analysis, recombinant protein expression, protein purification, WB analysis, cell-based cytotoxicity assays, and molecular binding stability measurement in order to identify candidate drug molecules that can inhibit the Syk enzyme, which is one of the potential and versatile targets for the treatment of AML. This approach differs from common drug development processes in that it integrates *in silico* approaches with experimental laboratory processes. In addition, it parallels other modern approaches of this kind in the literature.

Initially, among the inhibitors and candidate molecules in the opnMe database, BI 1002494 molecule stood out due to its conformation fitting into the ATP binding pocket and its high binding affinity (-8.2 kcal/mole). It was determined that the inhibitor established important molecular interactions such as hydrogen bonding with previously mentioned amino acid residues such as Arg498 and Lys458. These findings were found to be consistent with the reports on the binding modes of R406-like Syk enzyme inhibitors in the literature. Thus, BI 1002494 inhibitor has been concluded to be a strong candidate molecule for experimental tests. Furthermore, despite an approximately 25-fold difference between the IC50 values, the *in silico* binding affinity values are almost identical, suggesting that a direct relationship can't be established between binding affinity and IC50. A specific point to be discussed in the future is that the negative control (BI-2492) of BI 1002494 exhibited a binding affinity (-8.2 kcal/mole) comparable to that of the positive inhibitor, and the negative control groups showed remarkable cell death in MTT results.

In the next step, modified Syk protein was produced recombinantly in *Escherichia coli* bacterium BL21(DE3) strain using pET-28a vector and the protein in question was purified by His-tag Ni-NTA affinity chromatography method. The effectiveness of the purification protocol and IPTG induction conditions has been confirmed by SDS-PAGE experiments, as the protein with a molecular weight of ~33 kDa gave clear band results in the expected size. Continuous determination of protein concentrations with BCA tests has ensured equal loading in each well in SDS-PAGE and WB experiments. These verification methods and steps play a key role in the verification of recombinant protein

production and the reliability of subsequent experiments. Moreover, despite the risk of toxicity that may arise when kinase enzymes are produced in high quantities alone, it was also understood that the recombinantly produced protein in the study doesn't have a toxic effect on the bacterial strain as a result of its production. Finally, the increase in T_m detected in recombinantly produced Syk samples exposed to BI 1002494 inhibitor through TSA analyses has been accepted as a strong scientific data confirming the molecular interaction between the inhibitor and the target protein recombinantly produced.

Cytotoxicity experiments conducted with MTT showed that the candidate molecule BI 1002494 showed reasonable dose-dependent cytotoxic effects in the AML cell line MOLM-13, but, as expected, didn't cause significant proliferation inhibition in the CML cell line K562. This finding supported the findings of studies that AML cells are more sensitive to the inhibitor due to high Syk expression and FLT3-ITD mutation. On the other hand, the relatively low sensitivity of the CML cell line K562 to Syk inhibition is consistent with both the findings and expectations.

In summary, this study adopts an interdisciplinary approach that is not widely available in the literature by comprehensively integrating *in silico* drug discovery, recombinant protein production and cell-based pharmacological methods. The findings in the study prove that BI 1002494 molecule is a reasonable candidate for preclinical studies as a Syk enzyme inhibitor in AML disease. The findings and the study itself contribute to the development of new targeted therapeutic approaches.

Chapter 4

Conclusions and Future Prospects

4.1 Conclusions

This study, with its comprehensive and detailed analyses and experiments, demonstrates the importance of multidisciplinary approaches for the discovery of novel inhibitors targeting the catalytic domain of Syk, an enzyme that plays a significant role in AML. In the first step, *in silico* analyses of candidate molecules in the opnMe database determined that BI 1002494 inhibitor exhibited high binding affinity (-8.2 kcal/mole) to the catalytic domain of Syk. Molecular docking findings revealed that BI 1002494 inhibitor provides binding stability by forming molecular interactions with amino acid residues such as Leu377, which have been shown to bind to it in previous studies. These findings, when compared with the findings of known drugs such as R406, which have been shown to be important in previous studies, indicate that the BI 1002494 inhibitor has an alternative and unique drug profile for AML disease, thus enabling a drug repurposing study for BI 1002494.

After molecular docking findings and identification of the candidate molecule, sequences encoding the ATP-binding site and interdomain B regions of the Syk protein were inserted into the pET-28a vector. Thus, high amounts of recombinant protein were produced by IPTG induction in BL21(DE3) bacteria. The presence of recombinant proteins purified by His-tag Ni-NTA affinity chromatography was confirmed by SDS-PAGE and WB. Furthermore, the binding of the candidate molecule to the recombinantly produced Syk protein was analyzed using TSA. The findings revealed a significant increase in the T_m of the protein when combined with the inhibitor, indicating strong binding between the protein and the inhibitor.

MTT cytotoxicity assays on AML and CML cells reported that the inhibitor BI 1002494 exhibited a proliferation-suppressive effect on the AML model cell line MOLM-13, consistent with the dose level. Analysis of the experimental data revealed an IC50 value of 1036 nM, indicating a ~25 times lower potency compared to the FDA-approved drug R406. However, other pharmacokinetic properties of the candidate molecule, its structural framework, and the fact that it was first tested on AML in the literature suggest that the inhibitor carries novel value in terms of drug repurposing. Furthermore, the absence of cytotoxic effects on the control cell line K562, as expected, confirmed the inhibitor's cell type selectivity.

The combined use of *in silico* analyses, TSA, WB assays, and cytotoxicity tests in this study clearly demonstrates the importance of multi-layered validation approaches in generating reliable findings and cross-validation in drug discovery and drug repurposing processes. Furthermore, the methodological protocols employed in this study are applicable not only to the discovery of Syk candidate inhibitors but also to the identification of novel kinase targets with similar structural and functional properties. From this perspective, this study and its findings have the potential to serve as a reference for academic research in the development of targeted therapies in the future.

In conclusion, the Syk inhibitor BI 1002494, with its unique binding profile targeting Syk, a key enzyme in AML, and its specific cytotoxic effects in AML cells, represents a strong drug candidate for preclinical studies. Thus, the integrated approaches presented in this study offer significant contributions to cancer research in developing novel, targeted therapies.

4.2 Societal Impact and Contribution to Global Sustainability

The findings in this study, all in accordance with academic methods, have significant potential for both societal impact and global sustainability. First, for AML, a type of cancer with serious, high mortality rate, and limited targeted therapeutic options, the use of BI 1002494 as a potential Syk enzyme inhibitor offers a novel therapeutic candidate. Directly addressing this molecule in ongoing preclinical and clinical studies

will likely contribute to key areas such as improving the quality of life and increasing current survival rates in AML patients who have developed drug resistance over time. Thus, this potential impact directly aligns with public health interests in developing effective treatment strategies for cancers with poor prognostic profiles.

From a scientific and academic perspective, the study's methodological strategy and planning contribute to sustainability and ethical values. For instance, prioritizing *in silico* molecular docking screening and candidate molecule screening approaches, and the findings derived from these approaches, before laboratory experiments, reduces the number of candidate molecules that need to be tested biologically in the laboratory. This minimizes resource consumption and potential chemical waste issues, while also minimizing animal and human use, which are crucial steps in drug discovery processes. In this context, these approaches also implement the principles of Replacement, Reduction and Refinement (3R), which directly address ethical responsibility in scientific research. Furthermore, recombinant protein production with high yield in bacterial systems such as *Escherichia coli* BL21(DE3) allows for a cost-effective and reduced environmental footprint compared to other expression systems (e.g., mammalian cell expression systems). This approach is both scalable and creates potential opportunities for laboratories and countries with limited budgets, increasing the accessibility of such studies.

Another, and perhaps most important, sustainable societal contribution of the study is the use of the previously mentioned drug repurposing approach as a key approach. Using inhibitors like BI 1002494, whose pharmacological profile and properties have been established in previous scientific studies and are currently being studied in the preclinical setting and have a high probability of future approval from reputable organizations like the FDA, with the repurposing approach allows bypassing many of the tedious *de novo* drug development stages. This accelerates clinical processes and minimizes overall costs. This drug repurposing approach is particularly critical for laboratories and countries where access to new therapeutics is limited due to economic constraints. In conclusion, this study and its findings offer significant contributions not only to targeted therapy research for AML but also to ethical and globally sustainable drug discovery.

4.3 Future Prospects

The integration of *in silico* and *in vitro* approaches successfully implemented in this study and the resulting findings suggest several future steps that will strengthen the potential of the BI 1002494 inhibitor as a novel anti-AML drug. First, a more comprehensive selectivity analysis of the inhibitor can be conducted to more comprehensively and definitively determine the candidate molecule's potential effects beyond the Syk enzyme and AML cells, thus confirming the inhibitor's target specificity. For this confirmation, comprehensive kinase and cell type screening assays would provide pharmacological data to support the inhibitor's clinical validity. Moreover, in light of the data obtained from *in silico* analyses of the inhibitor, some modifications to the skeleton structure may provide improvements for the previously mentioned IC50 values (in comparison with R406).

Future pharmacodynamic and pharmacokinetic studies addressing important points such as metabolic stability, half-life, and systemic toxicity of the candidate molecule would provide critical data on the suitability of the molecule for *in vivo* applications. Detailed molecular dynamics (MD) analysis studies could also provide detailed data on the conformational stability of the candidate molecule BI 1002494 in the ATP-binding region of Syk. This could reveal induced-fit effects and possible flexible interactions that are not detected by standard molecular docking analyses.

Furthermore, the extent to which including a portion of the "Interdomain B" domain of the recombinant protein would impact binding affinity can be assessed in a future comparative study using only the catalytic domain of Syk. Thus, a comparison based on TSA findings could provide data on the potential effects of modification of the candidate molecule, and even its use in complex with other drugs, on diseases such as AML. In this context, the possibility of using inhibitors like BI 1002494 with other drugs to prevent drug resistance and potentially neutralize other signaling pathways is another point worth considering in future studies.

The "leaky expression" phenomenon encountered in the study findings, which indicates the production of protein in small amounts without the addition of IPTG, is also a topic worthy of future study. The presence of the DNA sequence necessary to produce

the protein in question within the bacteria may lead to recombinant production of the protein, despite the presence of IPTG, and investigating this phenomenon is crucial for recombinant protein production research.

It is highly recommended that proteins in Syk-dependent pathways, such as STAT5 and IκBα, and their phosphorylation levels after the treatment with certain drug doses be tracked with WB experiments.

Finally, *in vivo* studies are recommended for the BI 1002494 inhibitor. *In vivo* studies in transgenic mouse models would confirm the inhibitory efficacy and safety reported in *in vitro* experiments, thus enabling the inhibitor to progress to phase I clinical trials.

BIBLIOGRAPHY

[1] Döhner, H., Wei, A. H., Appelbaum, F. R., Craddock, C., DiNardo, C. D., Dombret, H., Ebert, B. L., Fenaux, P., Godley, L. A., Hasserjian, R. P., Larson, R. A., Levine, R. L., Miyazaki, Y., Niederwieser, D., Ossenkoppele, G., Röllig, C., Sierra, J., Stein, E. M., Tallman, M. S., . . . Löwenberg, B. (2022). Diagnosis and management of aml in adults: 2022 recommendations from an international expert panel on behalf of the ELN. *Blood*, *140*(12), 1345–1377. https://doi.org/10.1182/blood.2022016867

[2] Papaemmanuil, E., Gerstung, M., Bullinger, L., Gaidzik, V. I., Paschka, P., Roberts, N. D., Potter, N. E., Heuser, M., Thol, F., Bolli, N., Gundem, G., Van Loo, P., Martincorena, I., Ganly, P., Mudie, L., McLaren, S., O'Meara, S., Raine, K., Jones, D. R., . . . Campbell, P. J. (2016). Genomic classification and prognosis in acute myeloid leukemia. *New England Journal of Medicine*, *374*(23), 2209–2221. https://doi.org/10.1056/nejmoa1516192

[3] Ley, T. J., Ding, L., Walter, M. J., McLellan, M. D., Lamprecht, T., Larson, D. E., Kandoth, C., Payton, J. E., Baty, J., Welch, J., Harris, C. C., Lichti, C. F., Townsend, R. R., Fulton, R. S., Dooling, D. J., Koboldt, D. C., Schmidt, H., Zhang, Q., Osborne, J. R., . . . Wilson, R. K. (2010). DNMT3A mutations in acute myeloid leukemia. *New England Journal of Medicine*, *363*(25), 2424–2433. https://doi.org/10.1056/nejmoa1005143

[4] Stirewalt, D. L., & Radich, J. P. (2003). The role of FLT3 in haematopoietic malignancies. *Nature Reviews. Cancer*, *3*(9), 650–665. https://doi.org/10.1038/nrc1169

[5] Chua, C. C., Loo, S., Reynolds, J., Tiong, I. S., Fong, C. Y., Ting, S. B., Fleming, S., Roberts, A. W., & Wei, A. H. (2022). High response and prolonged treatment-free remission after a short-course of modified intensive chemotherapy and venetoclax in elderly aml: An updated analysis of the caveat trial. *Blood*, *140*(Supplement 1), 1708–1710. https://doi.org/10.1182/blood-2022-165021

[6] Shao, X., Xu, A., Du, W., Xu, T., Huang, Y., Xia, Z., Wang, W., Cai, M., Zhang, X., Zhang, J., Cao, J., Xu, X., Yang, B., He, Q., & Ying, M. (2023). Palmitoyltransferase ZDHHC21 regulates oxidative phosphorylation to induce differentiation block and stemness in AML. *Blood*. https://doi.org/10.1182/blood.2022019056

[7] Narayanan, S., Wu, Z., Wang, J., Ma, H., Acharekar, N., Koya, J., Yoganathan, S., Fang, S., Chen, Z., & Pan, Y. (2021). The spleen tyrosine kinase inhibitor, entospletinib (GS-9973) restores chemosensitivity in lung cancer cells by modulating ABCG2-mediated multidrug resistance. *International Journal of Biological Sciences*, *17*(10), 2652–2665. https://doi.org/10.7150/ijbs.61229

[8] Polak, A., Bialopiotrowicz, E., Krzymieniewska, B., Wozniak, J., Stojak, M., Cybulska, M., Kaniuga, E., Mikula, M., Jablonska, E., Gorniak, P., Noyszewska-Kania, M., Szydlowski, M., Piechna, K., Piwocka, K., Bugajski, L., Lech-Maranda, E., Barankiewicz, J., Kolkowska-Lesniak, A., Patkowska, E., . . . Juszczynski, P. (2020). SYK inhibition targets acute myeloid leukemia stem cells by blocking their

oxidative metabolism. *Cell Death and Disease*, *11*(11). https://doi.org/10.1038/s41419-020-03156-8

[9] Gonzalez, M. W., & Kann, M. G. (2012). Chapter 4: Protein Interactions and Disease. *PLoS Computational Biology*, *8*(12), e1002819. https://doi.org/10.1371/journal.pcbi.1002819

[10] Ali, A., & Bagchi, A. (2015). An overview of Protein-Protein interaction. *Current Chemical Biology*, *9*(1), 53–65. https://doi.org/10.2174/2212796809011511091611 26

[11] Titeca, K., Lemmens, I., Tavernier, J., & Eyckerman, S. (2018). Discovering cellular protein-protein interactions: Technological strategies and opportunities. *Mass Spectrometry Reviews*, *38*(1), 79–111. https://doi.org/10.1002/mas.21574

[12] Laraia, L., McKenzie, G., Spring, D. R., Venkitaraman, A. R., & Huggins, D. J. (2015). Overcoming chemical, biological, and computational challenges in the development of inhibitors targeting Protein-Protein interactions. *Chemistry & Biology*, *22*(6), 689–703. https://doi.org/10.1016/j.chembiol.2015.04.019

[13] Robinson, P. K. (2015). Enzymes: principles and biotechnological applications. *Essays in Biochemistry*, *59*, 1–41. https://doi.org/10.1042/bse0590001

[14] Buljan, M., Ciuffa, R., Van Drogen, A., Vichalkovski, A., Mehnert, M., Rosenberger, G., Lee, S., Varjosalo, M., Pernas, L. E., Spegg, V., Snijder, B., Aebersold, R., & Gstaiger, M. (2020). Kinase interaction network expands functional and disease roles of human kinases. *Molecular Cell*, *79*(3), 504-520.e9. https://doi.org/10.1016/j.molcel.2020.07.001

[15] Neagu, M., & Constantin, C. (2021). Signal transduction in immune cells and protein kinases. In *Advances in experimental medicine and biology* (pp. 133–149). https://doi.org/10.1007/978-3-030-49844-3_5

[16] Fabbro, D., Cowan-Jacob, S. W., & Moebitz, H. (2015). Ten things you should know about protein kinases: IUPHAR Review 14. *British Journal of Pharmacology*, *172*(11), 2675–2700. https://doi.org/10.1111/bph.13096

[17] Paul, M. K., & Mukhopadhyay, A. K. (2004). Tyrosine kinase – Role and significance in Cancer. *International Journal of Medical Sciences*, 101–115. https://doi.org/10.7150/ijms.1.101

[18] Chehayeb, R. J., & Boggon, T. J. (2020). SH2 Domain binding: diverse FLVRs of Partnership. *Frontiers in Endocrinology*, *11*. https://doi.org/10.3389/fendo.2020.575220

[19] BioRender. (n.d.). Representation of the working principle of tyrosines kinase. BioRender. Retrieved July 8, 2025, from https://app.biorender.com

[20] Braselmann, S., Taylor, V., Zhao, H., Wang, S., Sylvain, C., Baluom, M., Qu, K., Herlaar, E., Lau, A., Young, C., Wong, B. R., Lovell, S., Sun, T., Park, G., Argade, A., Jurcevic, S., Pine, P., Singh, R., Grossbard, E. B., . . . Masuda, E. S. (2006). R406, an orally available spleen tyrosine kinase inhibitor blocks FC receptor signaling and reduces immune complex-mediated inflammation. *Journal of Pharmacology and Experimental Therapeutics*, *319*(3), 998–1008. https://doi.org/10.1124/jpet.106.109058

[21] Mócsai, A., Ruland, J., & Tybulewicz, V. L. J. (2010). The SYK tyrosine kinase: a crucial player in diverse biological functions. *Nature Reviews. Immunology*, *10*(6), 387–402. https://doi.org/10.1038/nri2765

[22] Wagner, M. J., Stacey, M. M., Liu, B. A., & Pawson, T. (2013). Molecular mechanisms of SH2- and PTB-domain-containing proteins in receptor tyrosine kinase signaling. *Cold Spring Harbor Perspectives in Biology*, *5*(12), a008987. https://doi.org/10.1101/cshperspect.a008987

[23] Bhullar, K. S., Lagarón, N. O., McGowan, E. M., Parmar, I., Jha, A., Hubbard, B. P., & Rupasinghe, H. P. V. (2018). Kinase-targeted cancer therapies: progress, challenges and future directions. *Molecular Cancer*, *17*(1). https://doi.org/10.1186/s12943-018-0804-2

[24] Rao, S., Liu, X., Freedman, B. D., & Behrens, E. M. (2013). Spleen Tyrosine Kinase (Syk)-dependent Calcium Signals Mediate Efficient CpG-induced Exocytosis of Tumor Necrosis Factor α (TNFα) in Innate Immune Cells. *Journal of Biological Chemistry*, *288*(18), 12448–12458. https://doi.org/10.1074/jbc.m113.454405

[25] Oellerich, T., Mohr, S., Beck, J., Bohnenberger, H., Doebele, C., Corso, J., Bug, G., Schuetz, E., Urlaub, H., & Serve, H. (2014). Syk and btk transduce survival and proliferation-inducing signals by activating distinct signaling pathways and transcriptional programs in aml cells. *Blood*, *124*(21), 3594. https://doi.org/10.1182/blood.v124.21.3594.3594

[26] Marchetti, G., Dessì, A., Dallocchio, R., Tsamesidis, I., Pau, M. C., Turrini, F. M., & Pantaleo, A. (2020). Syk inhibitors: new computational insights into their intraerythrocytic action in plasmodium falciparum malaria. *International Journal of Molecular Sciences*, *21*(19), 7009. https://doi.org/10.3390/ijms21197009

[27] Lamb, D. J., Wollin, S. L., Schnapp, A., Bischoff, D., Erb, K. J., Bouyssou, T., Guilliard, B., Strasser, C., Wex, E., Blum, S., Thaler, E., Nickel, H., Radmacher, O., Haas, H., Swantek, J. L., Souza, D., Canfield, M., White, D., Panzenbeck, M., . . . Hoffmann, M. (2016). BI 1002494, a novel potent and selective oral spleen tyrosine kinase inhibitor, displays differential potency in human basophils and B cells. *Journal of Pharmacology and Experimental Therapeutics*, *357*(3), 554–561. https://doi.org/10.1124/jpet.116.233155

[28] Deshpande, S. H., Muhsinah, A. B., Bagewadi, Z. K., Ankad, G. M., Mahnashi, M. H., Yaraguppi, D. A., Shaikh, I. A., Khan, A. A., Hegde, H. V., & Roy, S. (2023). In silico study on the Interactions, molecular docking, dynamics and simulation of potential compounds from withania somnifera (L.) dunal root against cancer by targeting KAT6A. *Molecules*, *28*(3), 1117. https://doi.org/10.3390/molecules28031117

[29] Ganjoo, A., & Prabhakar, C. (2019). In silico structural anatomization of spleen tyrosine kinase inhibitors: pharmacophore modeling, 3D QSAR analysis and molecular docking studies. *Journal of Molecular Structure*, *1189*, 102–111. https://doi.org/10.1016/j.molstruc.2019.04.009

[30] Trott, O., & Olson, A. J. (2009). AutoDock vina: improving the speed and accuracy of docking with a new scoring function, efficient optimization, and multithreading. *Journal of Computational Chemistry*, *31*(2), 455–461. https://doi.org/10.1002/jcc.21334

[31] Boehringer Ingelheim. (2017). *opnMe: Boehringer Ingelheim open innovation portal*. opnMe. https://www.opnme.com

[32] Gollner, A., Heine, C., & Hofbauer, K. S. (2023). Kinase Degraders, Activators, and Inhibitors: Highlights and synthesis routes to the chemical probes on OpnMe.com, Part 1. *ChemMedChem*, *18*(10). https://doi.org/10.1002/cmdc.202300031

[33] Tabeling, C., Herbert, J., Hocke, A. C., Lamb, D. J., Wollin, S. L., Erb, K. J., Boiarina, E., Movassagh, H., Scheffel, J., Doehn, J. M., Hippenstiel, S., Maurer, M., Gounni, A. S., Kuebler, W. M., Suttorp, N., & Witzenrath, M. (2016). Spleen tyrosine kinase inhibition blocks airway constriction and protects from Th2-induced airway inflammation and remodeling. *Allergy*, *72*(7), 1061–1072. https://doi.org/10.1111/all.13101

[34] Van Eeuwijk, J. M., Stegner, D., Lamb, D. J., Kraft, P., Beck, S., Thielmann, I., Kiefer, F., Walzog, B., Stoll, G., & Nieswandt, B. (2016). The novel oral SYK inhibitor, BL1002494, protects mice from arterial thrombosis and thromboinflammatory brain infarction. *Arteriosclerosis Thrombosis and Vascular Biology*, *36*(6), 1247–1253. https://doi.org/10.1161/atvbaha.115.306883

[35] Grädler, U., Schwarz, D., Dresing, V., Musil, D., Bomke, J., Frech, M., Greiner, H., Jäkel, S., Rysiok, T., Müller-Pompalla, D., & Wegener, A. (2012). Structural and biophysical characterization of the SYK Activation Switch. *Journal of Molecular Biology*, *425*(2), 309–333. https://doi.org/10.1016/j.jmb.2012.11.007

[36] Şansaçar, M., Sarı, C., Yücel, M. S., Akçok, E. B. G., & Akçok, İ. (2025). Discovery of new candidates targeting the SH2 domains of spleen tyrosine kinase (SYK) through in silico studies. *ChemistrySelect*, *10*(22). https://doi.org/10.1002/slct.202500547

[37] O'Boyle, N. M., Banck, M., James, C. A., Morley, C., Vandermeersch, T., & Hutchison, G. R. (2011). Open Babel: An open chemical toolbox. *Journal of Cheminformatics*, *3*(1). https://doi.org/10.1186/1758-2946-3-33

[38] Vanommeslaeghe, K., Hatcher, E., Acharya, C., Kundu, S., Zhong, S., Shim, J., Darian, E., Guvench, O., Lopes, P., Vorobyov, I., & Mackerell, A. D. (2009). CHARMM general force field: A force field for drug-like molecules compatible with the CHARMM all-atom additive biological force fields. *Journal of Computational Chemistry*, *31*(4), 671–690. https://doi.org/10.1002/jcc.21367

[39] Koes, D. R., Baumgartner, M. P., & Camacho, C. J. (2013). Lessons Learned in Empirical Scoring with smina from the CSAR 2011 Benchmarking Exercise. *Journal of Chemical Information and Modeling*, *53*(8), 1893–1904. https://doi.org/10.1021/ci300604z

[40] Rezvani, S., Ebadi, A., & Razzaghi-Asl, N. (2021). In silico identification of potential Hsp90 inhibitors via ensemble docking, DFT and molecular dynamics simulations. *Journal of Biomolecular Structure and Dynamics*, *40*(21), 10665–10676. https://doi.org/10.1080/07391102.2021.1947383

[41] Magwenyane, A. M., Ugbaja, S. C., Amoako, D. G., Somboro, A. M., Khan, R. B., & Kumalo, H. M. (2022). Heat Shock Protein 90 (HSP90) Inhibitors as Anticancer Medicines: A Review on the Computer-Aided Drug Discovery Approaches over the Past Five Years. *Computational and Mathematical Methods in Medicine*, *2022*, 1–20. https://doi.org/10.1155/2022/2147763

[42] Mansueto, M. S., Reens, A., Rakhilina, L., Chi, A., Pan, B., & Miller, J. R. (2019). A reevaluation of the spleen tyrosine kinase (SYK) activation mechanism. *Journal of Biological Chemistry*, *294*(19), 7658–7668. https://doi.org/10.1074/jbc.ra119.008045

[43] Schindler, T., Sicheri, F., Pico, A., Gazit, A., Levitzki, A., & Kuriyan, J. (1999). Crystal Structure of Hck in Complex with a Src Family–Selective Tyrosine Kinase Inhibitor. *Molecular Cell*, *3*(5), 639–648. https://doi.org/10.1016/s1097-2765(00)80357-3

[44] Xu, W., Doshi, A., Lei, M., Eck, M. J., & Harrison, S. C. (1999). Crystal structures of C-SRC reveal features of its autoinhibitory mechanism. *Molecular Cell*, *3*(5), 629–638. https://doi.org/10.1016/s1097-2765(00)80356-1

[45] Young, M. A., Gonfloni, S., Superti-Furga, G., Roux, B., & Kuriyan, J. (2001). Dynamic Coupling between the SH2 and SH3 Domains of c-Src and Hck Underlies Their Inactivation by C-Terminal Tyrosine Phosphorylation. *Cell*, *105*(1), 115–126. https://doi.org/10.1016/s0092-8674(01)00301-4

[46] Deindl, S., Kadlecek, T. A., Brdicka, T., Cao, X., Weiss, A., & Kuriyan, J. (2007). Structural basis for the inhibition of tyrosine kinase activity of ZAP-70. *Cell*, *129*(4), 735–746. https://doi.org/10.1016/j.cell.2007.03.039

[47] Llc, G. B. (n.d.). *PET-28A(+) sequence and map*. SnapGene. https://www.snapgene.com/plasmids/pet_and_duet_vectors_(novagen)/pET-28a(%2B)

[48] Al-Muhanna, S. G., & Al-Muhanna, A. S. (2018). Construction and transformation of recombinant pET28a expression vector in BL21 (DE3) cells with basic bioinformatics analysis. Biochemistry and Cellular Archives, 18(1), 147–151. https://www.connectjournals.com/bca

[49] Shilling, P. J., Mirzadeh, K., Cumming, A. J., Widesheim, M., Köck, Z., & Daley, D. O. (2020). Improved designs for pET expression plasmids increase protein production yield in Escherichia coli. *Communications Biology*, *3*(1). https://doi.org/10.1038/s42003-020-0939-8

[50] Lorenz, T. C. (2012). Polymerase chain Reaction: basic protocol plus troubleshooting and optimization strategies. *Journal of Visualized Experiments*, *63*. https://doi.org/10.3791/3998

[51] Garibyan, L., & Avashia, N. (2013). Polymerase chain reaction. *Journal of Investigative Dermatology*, *133*(3), 1–4. https://doi.org/10.1038/jid.2013.1

[52] Walker, A., Taylor, J., Rowe, D., & Summers, D. (2008). A method for generating sticky-end PCR products which facilitates unidirectional cloning and the one-step assembly of complex DNA constructs. *Plasmid*, *59*(3), 155–162. https://doi.org/10.1016/j.plasmid.2008.02.002

[53] Rahimzadeh, M., Sadeghizadeh, M., Najafi, F., Arab, S., & Mobasheri, H. (2016). Impact of heat shock step on bacterial transformation efficiency. *PubMed*, *5*(4), 257–261. https://pubmed.ncbi.nlm.nih.gov/28261629

[54] Singh, M., Yadav, A., Ma, X., & Amoah, E. (2010). Plasmid DNA transformation in Escherichia Coli: effect of heat shock temperature, duration, and Cold Incubation of Ca[Cl.sub.2] treated cells. *International Journal of Biotechnology & Biochemistry*, *6*(4), 561+. https://link.gale.com/apps/doc/A323038265/AONE?u=anon~63eff478&sid=googleScholar&xid=166c0b08

[55] Tuttle, A. R., Trahan, N. D., & Son, M. S. (2021). Growth and Maintenance of Escherichia coli Laboratory Strains. *Current Protocols*, *1*(1). https://doi.org/10.1002/cpz1.20

[56] MACHEREY-NAGEL GmbH & Co. KG. (2023). *NucleoSpin® TriPrep: Total DNA, RNA, and protein isolation (User manual, Rev. 07)*. MACHEREY-NAGEL GmbH & Co. KG. https://www.mn-net.com

[57] New England Biolabs. (n.d.). *Restriction digest protocol* [Protocol]. New England Biolabs. Retrieved from https://www.neb.com

[58] New England Biolabs. (n.d.). *Optimizing restriction endonuclease reactions* [Protocol]. New England Biolabs. Retrieved from https://www.neb.com

[59] New England Biolabs. (n.d.). *Ligation protocol with T4 DNA ligase (M0202)* [Protocol]. New England Biolabs. https://www.neb.com

[60] Lee, P. Y., Costumbrado, J., Hsu, C., & Kim, Y. H. (2012). Agarose gel electrophoresis for the separation of DNA fragments. *Journal of Visualized Experiments*, *62*. https://doi.org/10.3791/3923

[61] Iacoviello, M. P., & Rubin, S. A. (2001). Sterile preparation of Antibiotic-Selective LB Agar plates using a microwave oven. *BioTechniques*, *30*(5), 963–965. https://doi.org/10.2144/01305bm08

[62] Upadhyay, S., Dhok, A., Agarkar, V., Kashikar, S., & Quazi, Z. S. (2024). A protocol for cloning, expression, and purification of Lysine exporter (LysE) gene of Mycobacterium tuberculosis. *F1000Research*, *12*, 297. https://doi.org/10.12688/f1000research.131768.3

[63] Bergkessel, M., & Guthrie, C. (2013). Colony PCR. *Methods in Enzymology on CD-ROM/Methods in Enzymology*, 299–309. https://doi.org/10.1016/b978-0-12-418687-3.00025-2

[64] Ashayeri-Panah, M., Eftekhar, F., Kazemi, B., & Joseph, J. (2017). *Cloning, optimization of induction conditions and purification of Mycobacterium tuberculosis Rv1733c protein expressed in Escherichia coli*. https://pmc.ncbi.nlm.nih.gov/articles/PMC5715279/

[65] Choi, T., & Geletu, T. T. (2018). High level expression and purification of recombinant flounder growth hormone in E. coli. *Journal of Genetic Engineering and Biotechnology*, *16*(2), 347–355. https://doi.org/10.1016/j.jgeb.2018.03.006

[66] Rizkia, P. R., Silaban, S., Hasan, K., Kamara, D. S., Subroto, T., Soemitro, S., & Maksum, I. P. (2015). Effect of isopropyl-β-D-thiogalactopyranoside concentration on prethrombin-2 recombinant gene expression in *Escherichia coli* ER2566. *Procedia Chemistry*, *17*, 118–124. https://doi.org/10.1016/j.proche.2015.12.121

[67] Li, L., Li, H., Tian, Q., Ge, B., Xu, X., Chi, Y., Zhao, H., Liu, Y., Jia, N., Zhou, T., Zhu, Y., & Zhou, Y. (2022). Expression and purification of soluble recombinant β-lactamases using Escherichia coli as expression host and pET-28a as cloning vector. *Microbial Cell Factories*, *21*(1). https://doi.org/10.1186/s12934-022-01972-5

[68] Lara, A. R., Galindo, J., Jaén, K. E., Juárez, M., & Sigala, J. (2020). Physiological Response of Escherichia coli W3110 and BL21 to the Aerobic Expression of Vitreoscilla Hemoglobin. *Journal of Microbiology and Biotechnology*, *30*(10), 1592–1596. https://doi.org/10.4014/jmb.2004.04030

[69] Ferdous, S., Dopp, J. L., & Reuel, N. F. (2021). Optimization of E. coli tip-sonication for high-yield cell-free extract using finite element modeling. *AIChE Journal*, *67*(10). https://doi.org/10.1002/aic.17389

[70] Budde, C., Schoenfish, M. J., Linder, M. E., & Deschenes, R. J. (2006). Purification and characterization of recombinant protein acyltransferases. *Methods*, *40*(2), 143–150. https://doi.org/10.1016/j.ymeth.2006.07.017

[71] Thermo Fisher Scientific. (2012). *HisPur™ Ni-NTA Superflow Agarose user guide*. Thermo Fisher Scientific Inc. https://www.thermofisher.com

[72] Spriestersbach, A., Kubicek, J., Schäfer, F., Block, H., & Maertens, B. (2015). Purification of His-Tagged proteins. *Methods in Enzymology on CD-ROM/Methods in Enzymology*, 1–15. https://doi.org/10.1016/bs.mie.2014.11.003

[73] Block, H., Maertens, B., Spriestersbach, A., Brinker, N., Kubicek, J., Fabis, R., Labahn, J., & Schäfer, F. (2009). Chapter 27 Immobilized-Metal Affinity Chromatography (IMAC). *Methods in Enzymology on CD-ROM/Methods in Enzymology*, 439–473. https://doi.org/10.1016/s0076-6879(09)63027-5

[74] Manns, J. M. (2011). SDS-Polyacrylamide gel electrophoresis (SDS-PAGE) of proteins. *Current Protocols in Microbiology*, *22*(1). https://doi.org/10.1002/9780471729259.mca03ms22

[75] Higashi, S. L., Yagyu, K., Nagase, H., Pearson, C. S., Geller, H. M., & Katagiri, Y. (2020). Ultra-High-Speed Western Blot using Immunoreaction Enhancing Technology. *Journal of Visualized Experiments*, *163*. https://doi.org/10.3791/61657

[76] Hanke, D., Brown, J. I., & Page, B. D. G. (2025). Thermal shift assays in drug discovery – Troubleshooting from biochemical to cellular applications. *Journal of Pharmacological and Toxicological Methods*, 108380. https://doi.org/10.1016/j.vascn.2025.108380

[77] Samuel, E. L. G., Holmes, S. L., & Young, D. W. (2021). Processing binding data using an open-source workflow. *Journal of Cheminformatics*, *13*(1). https://doi.org/10.1186/s13321-021-00577-1

[78] Bio-Rad Laboratories. (1998). *DC Protein Assay instruction manual (LIT448 Rev D)*. Bio-Rad Laboratories. Retrieved from https://www.bio-rad.com

[79] Sigma-Aldrich. (2013). *SYPRO® Orange Protein Gel Stain (Product information, Catalog Number S5692)*. Sigma-Aldrich Co. LLC. Retrieved from https://www.sigmaaldrich.com

[80] Lavinder, J. J., Hari, S. B., Sullivan, B. J., & Magliery, T. J. (2009). High-throughput thermal scanning: A general, rapid dye-binding thermal shift screen for protein engineering. *Journal of the American Chemical Society*, *131*(11), 3794–3795. https://doi.org/10.1021/ja8049063

[81] Cheng, C., Liu, M., Gao, X., Wu, D., Pu, M., Ma, J., Quinn, R. J., Xiao, Z., & Liu, Z. (2022). Identifying new ligands for JNK3 by fluorescence thermal shift assays and native mass spectrometry. *ACS Omega*, *7*(16), 13925–13931. https://doi.org/10.1021/acsomega.2c00340

[82] Wu, T., Hornsby, M., Zhu, L., Yu, J. C., Shokat, K. M., & Gestwicki, J. E. (2023). Protocol for performing and optimizing differential scanning fluorimetry experiments. *STAR Protocols*, *4*(4), 102688. https://doi.org/10.1016/j.xpro.2023.102688

[83] Bio-Rad Laboratories, Inc. (2022). *Protein thermal shift assays made easy with the Bio-Rad™ family of CFX real-time PCR systems* (Bulletin 7180). Bio-Rad Laboratories. Retrieved from https://www.bio-rad.com

[84] Janotka, Ľ., Messingerová, L., Šimoničová, K., Kavcová, H., Elefantová, K., Sulová, Z., & Breier, A. (2021). Changes in Apoptotic Pathways in MOLM-13 Cell Lines after Induction of Resistance to Hypomethylating Agents. *International Journal of Molecular Sciences*, *22*(4), 2076. https://doi.org/10.3390/ijms22042076

[85] Dutta, A., Sen, T., & Chatterjee, A. (2010, February 18). *Culture of K562 human myeloid leukemia cells in presence of fibronectin expresses and secretes MMP-9 in serum-free culture medium*. https://pmc.ncbi.nlm.nih.gov/articles/PMC2836506/

[86] Lim, S., Loh, H., Ting, K., Bradshaw, T. D., & Allaudin, Z. N. (2015). Reduction of MTT to purple formazan by vitamin E isomers in the absence of cells. *PubMed*, *26*(1), 111–120. https://pubmed.ncbi.nlm.nih.gov/26868595

[87] Seipel, K., Marques, M. A., Sidler, C., Mueller, B. U., & Pabst, T. (2018). MDM2- and FLT3-inhibitors in the treatment of FLT3-ITD acute myeloid leukemia, specificity and efficacy of NVP-HDM201 and midostaurin. *Haematologica, 103*(11), 1862–1872. https://doi.org/10.3324/haematol.2018.191650

[88] Moore, A. S., Faisal, A., De Castro, D. G., Bavetsias, V., Sun, C., Atrash, B., Valenti, M., De Haven Brandon, A., Avery, S., Mair, D., Mirabella, F., Swansbury, J., Pearson, A. D. J., Workman, P., Blagg, J., Raynaud, F. I., Eccles, S. A., & Linardopoulos, S. (2012). Selective FLT3 inhibition of FLT3-ITD+ acute myeloid leukaemia resulting in secondary D835Y mutation: a model for emerging clinical resistance patterns. *Leukemia*, *26*(7), 1462–1470. https://doi.org/10.1038/leu.2012.52

[89] Pasquet, J., Lagarde, V., & Mahon, F. (2015). Loss of SYK and LYN tyrosine kinase expression impair Ponatinib-Induced apoptosis in K562 cells. *Journal of Translational Proteomics Research*, *2*, 15–19. https://doi.org/10.15379/2410-3802.2015.02.3

[90] Riss, T. L., Moravec, R. A., Niles, A. L., Duellman, S., Benink, H. A., Worzella, T. J., & Minor, L. (2016, July 1). *Cell viability assays*. Assay Guidance Manual - NCBI Bookshelf. https://www.ncbi.nlm.nih.gov/books/NBK144065/

[91] Şansaçar, M., Pekin, Ö., & Gencer Akçok, E. B. (2024). Targeting HDAC enzymes by SAHA enhances the cytotoxic effects of cisplatin on acute myeloid leukemia cells. *Journal of Experimental and Clinical Medicine, 41*(3), 524–529. https://doi.org/10.52142/omujecm.41.3.14

[92] Boyraz, M. Ü., Shekhany, B., & Süzergöz, F. (2021). Cellular imaging analysis of MTT assay based on tetrazolium reduction. *Harran Üniversitesi Tıp Fakültesi Dergisi*, *18*(1), 95–99. https://doi.org/10.35440/hutfd.816390

[93] Kumar, V., Parate, S., Danishuddin, N., Zeb, A., Singh, P., Lee, G., Jung, T. S., Lee, K. W., & Ha, M. W. (2022). 3D-QSAR-Based pharmacophore modeling, virtual screening, and molecular dynamics simulations for the identification of spleen tyrosine kinase inhibitors. *Frontiers in Cellular and Infection Microbiology*, *12*. https://doi.org/10.3389/fcimb.2022.909111

[94] Akinnusi, P. A., Olubode, S. O., Adebesin, A. O., Alade, A. A., Nwoke, V. C., & Shodehinde, S. A. (2023). Optimal molecular binding data and pharmacokinetic profiles of novel potential triple-action inhibitors of chymase, spleen tyrosine kinase, and prostaglandin D2 receptor in the treatment of asthma. *Journal of Genetic Engineering and Biotechnology*, *21*(1), 113. https://doi.org/10.1186/s43141-023-00577-8

[95] Zhang, Y. (2016). Blue-white screening liquid can eliminate false positives in blue-white colony screening. *Genetics and Molecular Research*, *15*(2). https://doi.org/10.4238/gmr.15027925

[96] Nouemssi, S. B., Ghribi, M., Beauchemin, R., Meddeb-Mouelhi, F., Germain, H., & Desgagné-Penix, I. (2020). Rapid and Efficient Colony-PCR for High Throughput Screening of Genetically Transformed Chlamydomonas reinhardtii. *Life*, *10*(9), 186. https://doi.org/10.3390/life10090186

[97] Bell, J. R. (2008). A simple way to treat PCR products prior to sequencing using ExoSAP-IT ®. *BioTechniques*, *44*(6), 834. https://doi.org/10.2144/000112890

[98] New England Biolabs. (n.d.). *Protein expression using BL21(DE3) (C2527)* [Protocol]. New England Biolabs. Retrieved from https://www.neb.com

[99] Rozkov, A., & Enfors, S. (2004). Analysis and Control of Proteolysis of Recombinant Proteins in Escherichia coli. *Advances in Biochemical Engineering, Biotechnology*, 163–195. https://doi.org/10.1007/b95567

[100] Faas, R., Kiefer, D., Job, L., Pohle, A., Moß, K., Henkel, M., & Hausmann, R. (2017). Time-course and degradation rate of membrane scaffold protein (MSP1D1) during recombinant production. *Biotechnology Reports*, *17*, 45–48. https://doi.org/10.1016/j.btre.2017.12.003

[101] Francis, D. M., & Page, R. (2010). Strategies to Optimize Protein Expression in E. coli. *Current Protocols in Protein Science*, *61*(1). https://doi.org/10.1002/0471140864.ps0524s61

[102] Rosano, G. L., & Ceccarelli, E. A. (2014). Recombinant protein expression in Escherichia coli: advances and challenges. *Frontiers in Microbiology*, *5*. https://doi.org/10.3389/fmicb.2014.00172

[103] Galicia, M. E. D., Aldehaiman, A., Hong, S., Arold, S. T., & Grünberg, R. (2019). Methods for the recombinant expression of active tyrosine kinase domains: Guidelines and pitfalls. *Methods in Enzymology on CD-ROM/Methods in Enzymology*, 131–152. https://doi.org/10.1016/bs.mie.2019.02.027

[104] Singh, D., Rani, R., Rajendran, R., Kaur, N. J., Pandey, A., Chopra, P., Jain, T., Jain, M. K., Grover, S., Arya, R., & Saini, K. S. (2009). Human spleen tyrosine kinase (Syk) recombinant expression systems for high-throughput assays. *Biotechnology Journal*, *5*(2), 201–212. https://doi.org/10.1002/biot.200900139

[105] Michnik, A. (2003). Thermal stability of bovine serum albumin DSC study. *Journal of Thermal Analysis and Calorimetry*, *71*(2), 509–519. https://doi.org/10.1023/a:1022851809481

[106] Rombouts, I., Lagrain, B., Scherf, K. A., Lambrecht, M. A., Koehler, P., & Delcour, J. A. (2015). Formation and reshuffling of disulfide bonds in bovine serum albumin demonstrated using tandem mass spectrometry with collision-induced and electron-transfer dissociation. *Scientific Reports*, *5*(1). https://doi.org/10.1038/srep12210

[107] Jiang, B., Jain, A., Lu, Y., & Hoag, S. W. (2019). Probing Thermal Stability of Proteins with Temperature Scanning Viscometer. *Molecular Pharmaceutics*, *16*(8), 3687–3693. https://doi.org/10.1021/acs.molpharmaceut.9b00598

[108] Bradshaw, W. J., Harris, G., Gileadi, O., & Katis, V. L. (2024). The mechanism of allosteric activation of SYK kinase derived from multiple phospho-ITAM-bound structures. *Structure*. https://doi.org/10.1016/j.str.2024.09.024

[109] Thermo Fisher Scientific. (2021). *Protein Thermal Shift assay user guide* (Pub. No. MAN0025600 Rev. B.0). Thermo Fisher Scientific Inc.

[110] Bourgne, C., Janel, A., Chassagne, J., Rapatel, C., Tournilhac, O., Guerci, A., Lioret, F., BriançOn, A., Berger, J., Bamdad, M., Boiret-Dupre, N., & Berger, M. G. (2012). Phosphorylation of spleen tyrosine kinase (SYK) appears to be related to the blast phase of chronic myeloid leukemia. *Blood*, *120*(21), 4425. https://doi.org/10.1182/blood.v120.21.4425.4425

[111] Weisberg, E. L., Puissant, A., Stone, R., Sattler, M., Buhrlage, S. J., Yang, J., Manley, P. W., Meng, C., Buonopane, M., Daley, J. F., Lazo, S., Wright, R., Weinstock, D. M., Christie, A. L., Stegmaier, K., & Griffin, J. D. (2017). Characterization of midostaurin as a dual inhibitor of FLT3 and SYK and

potentiation of FLT3 inhibition against FLT3-ITD-driven leukemia harboring activated SYK kinase. *Oncotarget*, *8*(32), 52026–52044. https://doi.org/10.18632/oncotarget.19036

CURRICULUM VITAE

2018 – 2023	B.Sc., Molecular Biology and Genetics, Abdullah Gül University, Kayseri, TURKEY
2023 – 2025	M.Sc., Bioengineering, Abdullah Gül University, Kayseri, TURKEY